Shell-model states with seniority $\nu = 3$, 5, and 7 in odd-A neutron-rich Sn isotopes

Ł. W. Iskra,[1] R. Broda,[1] R. V. F. Janssens,[2] C. J. Chiara,[2,3,*] M. P. Carpenter,[2] B. Fornal,[1] N. Hoteling,[2,3] F. G. Kondev,[4] W. Królas,[1] T. Lauritsen,[2] T. Pawłat,[1] D. Seweryniak,[2] I. Stefanescu,[2,3] W. B. Walters,[3] J. Wrzesiński,[1] and S. Zhu[2]

[1]*Institute of Nuclear Physics, Polish Academy of Sciences, PL-31-342 Kraków, Poland*

[2]*Physics Division, Argonne National Laboratory, Argonne, Illinois 60439, USA*

[3]*Department of Chemistry and Biochemistry, University of Maryland, College Park, Maryland 20742, USA*

[4]*Nuclear Engineering Division, Argonne National Laboratory, Argonne, Illinois 60439, USA*

(Received 28 September 2015; published 7 January 2016)

Excited states with seniority $\nu = 3$, 5, and 7 have been investigated in odd neutron-rich ^{119,121,123,125}Sn isotopes produced by fusion-fission of 6.9-MeV/A ^{48}Ca beams with ^{208}Pb and ^{238}U targets and by fission of a ^{238}U target bombarded with 6.7-MeV/A ^{64}Ni beams. Level schemes have been established up to high spin and excitation energies in excess of 6 MeV, based on multifold gamma-ray coincidence relationships measured with the Gammasphere array. In the analysis, the presence of isomers was exploited to identify gamma rays and propose transition placements using prompt and delayed coincidence techniques. Gamma decays of the known $27/2^-$ isomers were expanded by identifying new deexcitation paths feeding $23/2^+$ long-lived states and $21/2^+$ levels. Competing branches in the decay of $23/2^-$ states toward two $19/2^-$ levels were delineated as well. In ^{119}Sn, a new $23/2^+$ isomer was identified, while a similar $23/2^+$ long-lived state, proposed earlier in ^{121}Sn, has now been confirmed. In both cases, isomeric half-lives were determined with good precision. In the range of $\nu = 3$ excitations, the observed transitions linking the various states enabled one to propose with confidence spin-parity assignments for all the observed states. Above the $27/2^-$ isomers, an elaborate structure of negative-parity levels was established reaching the $(39/2^-)$, $\nu = 7$ states, with tentative spin-parity assignments based on the observed deexcitation paths as well as on general yrast population arguments. In all the isotopes under investigation, strongly populated sequences of positive-parity $(35/2^+)$, $(31/2^+)$, and $(27/2^+)$ states were established, feeding the $23/2^+$ isomers via cascades of three transitions. In the ^{121,123}Sn isotopes, these sequences also enabled the delineation of higher-lying levels, up to $(43/2^+)$ states. In ^{123}Sn, a short half-life was determined for the $(35/2^+)$ state. Shell-model calculations were carried out for all the odd Sn isotopes, from ^{129}Sn down to ^{119}Sn, and the results were found to reproduce the experimental level energies rather well. Nevertheless, some systematic deviations between calculated and experimental energies, especially for positive-parity states, point to the need to improve some of the two-body interactions used in calculations. The computed wave-function amplitudes provide for a fairly transparent interpretation of the observed level structures. The systematics of level energies over the broad $A = 117$–129 range of Sn isotopes displays a smooth decrease with mass A, and the observed regularity confirms most of the proposed spin-parity assignments. The systematics of the $B(E2)$ reduced transition probabilities extracted for the $23/2^+$ and $19/2^+$ isomers is discussed with an emphasis on the close similarity of the observed A dependence with that of the $E2$ transition rates established for other $\nu = 2$, 3, and 4 isomers in the Sn isotopic chain.

DOI: 10.1103/PhysRevC.93.014303

I. INTRODUCTION

Between the major shells defined by the proton and neutron magic numbers 50 and 82, nucleons are filling the $g_{7/2}$, $d_{5/2}$, $d_{3/2}$, $s_{1/2}$, $h_{11/2}$ single-particle levels. The structure of excited states arising within this relatively large configuration space can be studied separately for protons and neutrons over a long series of $N = 82$ isotones and $Z = 50$ isotopes, respectively. Experimental studies of the $N = 82$ isotones established proton states in all such nuclei above neutron-rich ^{132}Sn, up to the most neutron deficient of these, ^{154}Hf, which is located close to the proton drip line. A substantial energy separation was demonstrated between the first two and last three of these orbitals and this observation led to the proposed "magicity" of ^{146}Gd [1]. Above this $Z = 64$, $N = 82$ ^{146}Gd isotone, the yrast structure is dominated by the high-j, $h_{11/2}$ orbital, as can be inferred from the regular appearance of $\nu(h_{11/2})^n$ seniority-2 and -3 isomers. The dependence on mass number A of the $E2$ transition rates from these long-lived states reflects the filling of the $h_{11/2}$ proton orbital: This state is half-filled at $Z = 71$, as ^{153}Lu has the lowest $B(E2)$ transition rate [2]. For neutrons, at $Z = 50$, the single-particle levels are distributed more evenly and no trace of an $N = 64$ subshell closure was found. Nevertheless, in the Sn isotopes heavier than $A = 120$, isomers arising from $\nu(h_{11/2})^n$ neutron configurations have been observed in all the even ($I^\pi = 10^+$) and odd ($I^\pi = 27/2^-$) nuclei [3–8]. The corresponding $B(E2)$ reduced transition probabilities exhibit a regular, systematic change with A with the lowest value occurring in ^{123}Sn, herewith defining $N = 73$ as the half-filling of the neutron $h_{11/2}$ subshell [6,7].

Whereas the early studies enabled a rather straightforward shell-model interpretation of the seniority $\nu = 2$ and 3

*Present address: U.S. Army Research Laboratory, Adelphi, Maryland 20783, USA.

excitations, the investigation of higher seniority states represented a challenge for both experiment and theory. On the experimental side, the main issue was the selection of suitable reactions to populate the states of interest with yields appropriate for detailed gamma-spectroscopy studies. For theory, on the other hand, it was clear at the onset that large-scale shell-model calculations involving the full configuration space between $N = 50$ and 82 would be required to achieve a reasonably complete description of observed structures. For the proton cases, standard fusion-evaporation reactions proved adequate to identify seniority-4, 16^+, and 15^- states with respective $\nu(h_{11/2})^4$ and $\nu(h_{11/2})^3 d_{3/2}$ configurations in the ^{150}Er isotone [9]. In ^{151}Tm, a few transitions above the $27/2^-$ state have been established as well. However, such investigations have not yet been extended to higher-Z, $N = 82$ isotones and, above ^{154}Hf, i.e., close to the proton drip line, they may well become rather difficult. For the neutron cases, on the other hand, extensive studies can be performed with fusion-fission reactions populating neutron-rich Sn isotopes in high-statistics, coincidence experiments. Recently, the present collaboration has reported comprehensive results for the even neutron-rich $^{118-128}$Sn isotopes [10]. The large data sets also contained much new information on the odd-mass Sn isotopes and the results on the latter nuclei are the focus of the present paper.

In the entire series of Sn isotopes, the isotopic identification of families of gamma rays located above the known 10^+ and $27/2^-$ isomers was the crucial starting point for the data analysis. This identification was based primarily on the analysis of delayed-coincidence relationships and on conclusions drawn from observed cross-coincidences with transitions emitted from the complementary fission fragments. Subsequently, the level schemes of the even Sn isotopes were extended up to excitation energies of the order of 8 MeV [10]. In ^{120,122,124,126}Sn, 15^- and 13^- isomeric states were identified and their half-lives were determined. For these isomers, the behavior with A of the $B(E2)$ reduced transition probabilities was found to exhibit a striking resemblance with that established earlier for the 10^+ and $27/2^-$ states. Above the 15^- isomers, many levels with seniority $\nu = 6$ were also identified. The firm spin-parity assignments for the seniority $\nu = 4$ levels were proposed on the basis of the decay paths from the 15^- long-lived levels to the 10^+, 8^+, and 7^- states. Shell-model calculations carried out for the even $^{122-130}$Sn isotopes confirmed these assignments and reproduced the measured level energies rather well. Following the work of Ref. [10], results of similar identifications and analyses are now presented here for high-spin states in the odd ^{119,121,123,125}Sn isotopes. As the overall approach is the same as in Ref. [10], experimental details are summarized only briefly and the main focus is placed squarely on the results and their interpretation.

As already mentioned in Ref. [10], an independent investigation, with objectives similar to those of the present work, was carried out by Astier *et al.* [11]. Level schemes above the 10^+ and $27/2^-$ isomers were presented for the even- and odd-Sn isotopes with $A = 119$–126. In this instance, the isotopes of interest were produced in ^{12}C + ^{238}U and ^{18}O + ^{208}Pb fusion-fission reactions. The agreement in the isotopic identifications and in the main parts of level schemes established in these parallel, independent experimental efforts can now also be extended to the odd Sn isotopes. However, as was the case for the even Sn nuclei [10], the present results extend significantly beyond those of Astier *et al.* [11], as additional transitions and new isomeric states have been identified. Furthermore, apart from the high-spin state structures, the present investigation also reports on a detailed study of the seniority $\nu = 3$ levels below the $27/2^-$ isomers, where new observations led to additional experimental information and a more complete interpretation.

II. EXPERIMENTAL PROCEDURES AND DATA ANALYSIS

The results presented below are based on data from three measurements performed at Argonne National Laboratory with heavy-ion beams from the ATLAS superconducting linear accelerator. Gamma rays were collected with the Gammasphere array [12], which consists of 101 Compton-suppressed, high-purity Ge detectors. In two of the experiments, a 330-MeV ^{48}Ca beam bombarded ^{208}Pb and ^{238}U targets and, in the third, the 430-MeV ^{64}Ni + ^{238}U reaction was employed. The beams were always pulsed with a 412-ns repetition rate and an intrinsic pulse width of about 0.3 ns. The targets had a thickness of $\sim$50 mg/cm^2, sufficient to stop the reaction products. Further details of the experimental procedures and analysis methods can be found in Ref. [10]; only their most important aspects are briefly outlined below.

Originally, most experiments were devoted to the study of neutron-rich nuclei produced in deep-inelastic reactions (e.g., [13–15]), however, the same data sets could be used to investigate a broad range of neutron-rich Sn isotopes produced with high yields by fission. The analysis of gamma-ray coincidence relationships, presented in Refs. [10,16,17], established unambiguously that, in the ^{48}Ca + ^{238}U and ^{48}Ca + ^{208}Pb systems, the Sn isotopes of interest were predominantly produced in fusion-fission reactions while, in the ^{64}Ni + ^{238}U reaction, the same nuclei were populated through fission of the ^{238}U target or of targetlike products. The relative populations of the known $27/2^-$ isomers were extracted from the coincidence data and are compared in Fig. 1 for the three reactions. The mass range of produced isotopes is similar in all cases and consistent with that given in Ref. [10] for the even Sn nuclei. It turned out that data from all three measurements could be used, herewith providing means to cross-check newly identified levels and transitions in the $^{119-125}$Sn isotopes presented here. While the analysis also included states below the $27/2^-$ isomers, the main focus was on establishing new structures above the long-lived states arising from $\nu > 3$ seniority excitations.

The delayed-coincidence technique was instrumental in identifying such structures in the ^{119,121,125}Sn isotopes as the $27/2^-$ isomeric half-lives are suitable for this purpose. On the other hand, the gamma cross-coincidence method was exploited in the case of ^{123}Sn in view of the longer (34 μs) half-life. Both techniques are described in Ref. [10] and will be outlined in the next section devoted to the presentation of the results for each isotope. However, before proceeding, it is useful to introduce the notation adopted in Ref. [10] to describe the coincidence data obtained under different

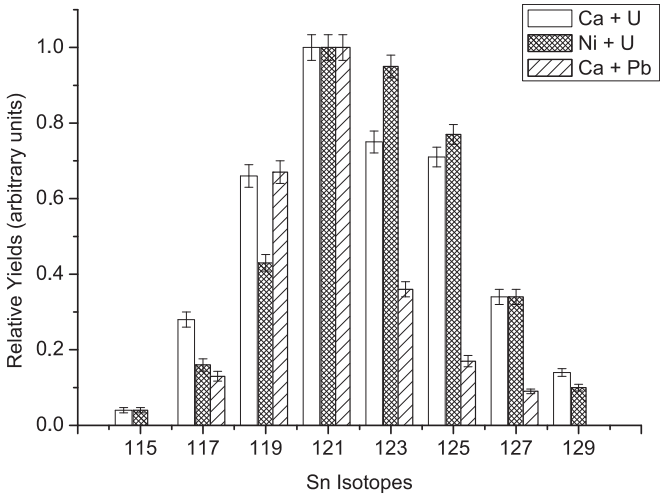

FIG. 1. Relative yields, in arbitrary units, for the Sn isotopes produced in the ^{48}Ca + ^{238}U, ^{64}Ni + ^{238}U, and ^{48}Ca + ^{208}Pb reactions described in the text. The yields were determined by using delayed coincidence data to estimate the population intensity of the $27/2^-$ isomers in each isotope.

time conditions. The 412-ns beam repetition rate, together with the intrinsic pulse width of ∼0.3 ns, provides a clear separation between the prompt (P) and delayed (D) gamma rays. Consequently, events were sorted into (PPP) and (DDD) coincidences cubes, as well as in (PDD) and (PPD) ones from which final spectra were obtained with appropriate energy and time gates. Time conditions for delayed transitions were optimized by taking into account the half-life of an isomeric state of interest in a specific level sequence. In some instances, involving sequential decay from two isomers, the (dDD) and (ddD) coincidence cubes were sorted by placing the delayed condition on the time parameter within shorter (d) and longer (D) time ranges, respectively. These symbols are used in the figures below to clarify the interpretation of the spectra provided as illustrations of the most salient features of the level schemes. It should be noted also that, in some part of the measurements, the event trigger, set in general to accept three- and higher-fold coincidence events, was changed to include twofold events as well so that decays from long-lived isomers involving only two coincident gamma transitions could be investigated. In the following, the results obtained for the odd $^{119-125}$Sn isotopes are described with an emphasis on new findings.

III. EXPERIMENTAL RESULTS

A. ^{119}Sn

Above the $11/2^-$, 89.5-keV, 293.1-d isomer, two long-lived states with respective half-lives and spin-parity values of 9.6(12) μs, $19/2^+$ and 34(10) ns, $27/2^-$ had been established previously [6,18]. Here, the large uncertainty on the half-life of the $27/2^-$ level has been reduced to 39(3) ns (see Sec. III E). The experimental information on ^{119}Sn yrast and near-yrast excitations has been significantly extended, as can be seen in the level scheme of Fig. 2. A new, 96(9)-ns, $23/2^+$ isomer was

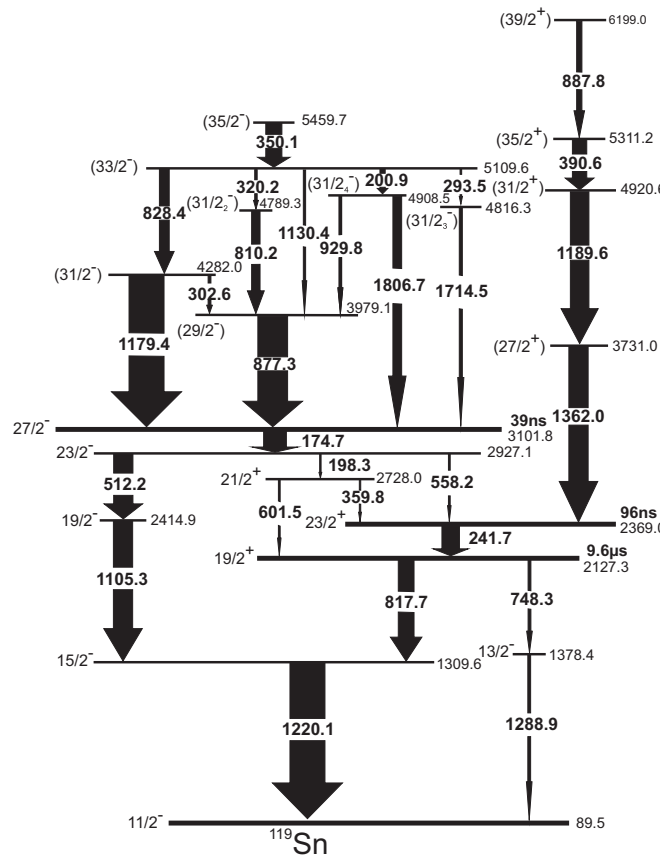

FIG. 2. The ^{119}Sn level scheme established in the present study. The arrow widths reflect the observed intensities for prompt and delayed transitions normalized separately. The spin-parity assignments are discussed in the text.

identified and the decay branches feeding it from the $27/2^-$, 39-ns state could be delineated. At higher excitation energy, many prompt gamma transitions were identified forming both an elaborate structure of levels above the $27/2^-$ isomer and an intense cascade of gamma rays populating the new $23/2^+$ long-lived level. The coincidence spectra documenting the most important findings are displayed in Fig. 3, and the energies and intensities of all the transitions in ^{119}Sn are listed in Table I.

In earlier work [6], the relative intensities of the 818-keV $M2$ and 748-keV $E3$ branches in the $19/2^+$, 9.6-μs isomer decay were not listed; therefore, the twofold coincidence data from the present experiments were used to provide this information (see Table I). The subsequent analysis was started with a search for the $I^\pi = 23/2^+$ isomer, as this level was anticipated, based on the expected analogy with observations in ^{121}Sn [11], ^{123}Sn [6], and ^{125}Sn [19], discussed also in the next subsections. The selective (dDD) data led to the observation of the delayed (d) 242- and 602-keV transitions, shown in Fig. 3(a) to precede in time the more delayed pair of gating (DD) 818-, 1220-keV gamma rays from the 9.6-μs isomer. The short time range defining the (d) delay reduced the intensity of the 242-keV line significantly in Fig. 3(a), as the latter turned out to be the isomeric transition from the $23/2^+$

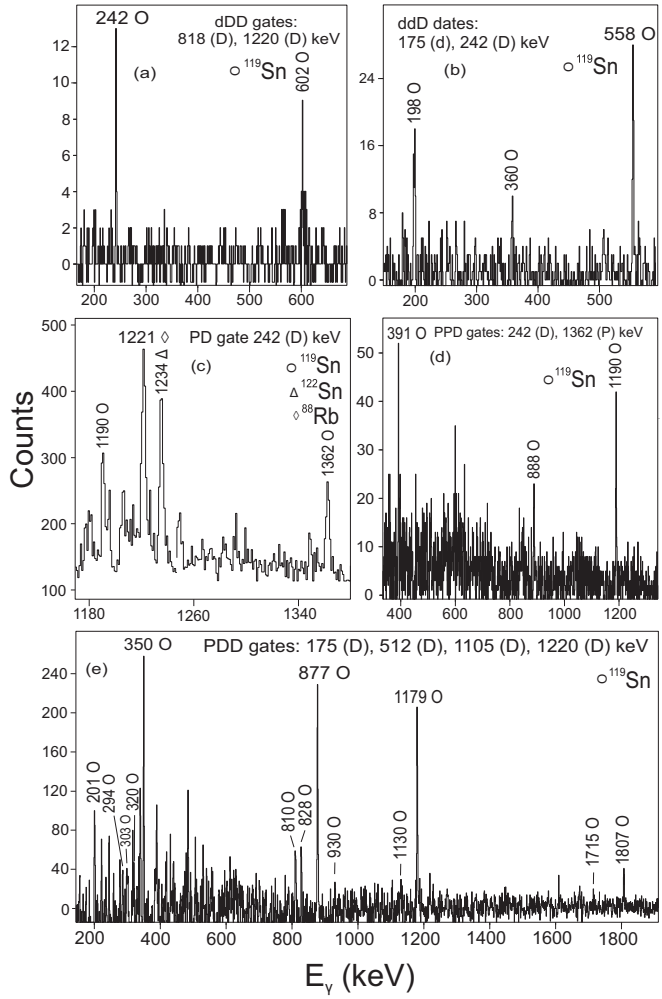

FIG. 3. Crucial coincidence spectra used to extend the ^{119}Sn level scheme. Gamma rays identified with ^{119}Sn are labeled with open circles. The short-delayed spectrum (a) documents transitions preceding in time the long-delayed (D) 818- and 1220-keV gamma rays, while the short-delayed spectrum (b) highlights the connection between $23/2^-$ and $23/2^+$ states. The next panels display prompt gamma rays located above the $23/2^+$ isomers, preceding in time the delayed (D) 242-keV transition (c) and with the more stringent condition of an additional prompt gate on the 1362-keV line (d). Finally, prompt spectrum (e) was obtained with delayed double coincidence gates placed on all pairs involving the 175-, 512-, 1105-, and 1220-keV gamma rays.

level characterized by the relatively long, 96(9)-ns half-life (see Sec. III E). This reduction resulted also in the absence in Fig. 3(a) of the much weaker 198-, 360-, and 558-keV transitions connecting the $23/2^+$ isomer with the known $27/2^-$ one (Fig. 2). However, these three lines are clearly visible in the coincidence spectrum of Fig. 3(b) obtained from the (ddD) cube with the requirement of a 175-keV gamma ray with a short (d) delay time (decay out of the $27/2^-$ isomer) preceding the 242-keV transition of longer (D) delay time out of the 96-ns, $23/2^+$ state. The expectations mentioned above, the half-life and the feeding from the $27/2^-$ isomer, all led to the unique $23/2^+$ spin-parity assignment for the new isomer at 2369 keV.

TABLE I. List of the levels identified in ^{119}Sn with their proposed spin-parity assignments. The last two columns include energies and relative intensities of the depopulating transitions as determined in the present study. The intensities of the delayed transitions have been normalized to the 1220-keV line defined as 100 units, while, for prompt transitions marked with an asterisk, this normalization refers to the 1179-keV transition.

E_{level} (keV)	I^π	E_γ (keV)	I_γ
89.5	$11/2^-$		
1309.6	$15/2^-$	1220.1(1)	100
1378.4	$13/2^-$	1288.9(2)	8(1)
2127.3	$19/2^+$	748.3(2)	8(1)
		817.7(1)	45(4)
2369.0	$23/2^+$	241.7(2)	50(4)
2414.9	$19/2^-$	1105.3(1)	55(4)
2728.0	$21/2^+$	359.8(3)	4(1)
		601.5(4)	1.0(3)
2927.1	$23/2^-$	198.3(3)	4(1)
		512.2(1)	55(5)
		558.2(3)	5(1)
3101.8	$27/2^-$	174.7(1)	64(4)
3731.0	$(27/2^+)$	1362.0(2)	55(5)*
3979.1	$(29/2^-)$	877.3(1)	85(7)*
4282.0	$(31/2^-)$	302.6(3)	8(3)*
		1179.4(1)	100*
4789.3	$(31/2_2^-)$	810.2(2)	24(5)*
4816.3	$(31/2_3^-)$	1714.5(5)	9(2)*
4908.5	$(31/2_4^-)$	929.8(4)	7(3)*
		1806.7(4)	25(6)*
4920.6	$(31/2^+)$	1189.6(2)	53(5)*
5109.6	$(33/2^-)$	200.9(2)	15(4)*
		293.5(4)	5(2)*
		320.2(3)	7(3)*
		828.4(1)	28(4)*
		1130.4(3)	7(2)*
5311.2	$(35/2^+)$	390.6(4)	41(4)*
5459.7	$(35/2^-)$	350.1(1)	46(5)*
6199.0	$(39/2^+)$	887.8(3)	15(2)*

Consequently, the additional new level at 2728 keV is assigned $I^\pi = 21/2^+$, as any other spin value could be excluded based on the observed transitions connecting this state with the $23/2^-$ level above it and with the $23/2^+$, $19/2^+$ states located below. The positive parity is consistent with both the absence of a decay branch to the $19/2^-$, 2415-keV state and with the small intensity of the 198-keV $E1$ branch from the $23/2^-$ level, as the latter gamma ray would compete more effectively with the 512-keV $E2$ transition if it was of $M1$ character. This positive parity is also in line with the results of calculations predicting no $21/2^-$ state at or near this excitation energy.

A new cascade of four prompt transitions was placed as feeding the $23/2^+$ isomer at 2369 keV. They were identified as preceding in time the delayed 242-keV gamma ray which was selected from the twofold (PD) matrices. The selectivity of this type of analysis is somewhat limited, but the inspection of spectra from all three experiments, nevertheless, provided an unambiguous identification. In Fig. 3(c), the high-energy part

of such a coincidence spectrum, from the ^{48}Ca + ^{208}Pb data, is displayed. The data provide evidence for the new 1362- and 1190-keV lines, although these are observed together with contaminant transitions associated with known isomeric decays which also happen to have a 242-keV gamma ray in their decay [see legend in Fig. 3(c)]. The (PP) matrix obtained from the (PPD) cube with a delayed (D) 242-keV gating transition clarified the entire 1362-1190-391-888-keV cascade into the $23/2^+$ isomer, and established the ordering of the transitions, based on decreasing intensities (see Table I): This is illustrated in Fig. 3(d) by the spectrum in coincidence with the 1362-keV line from this (PP) matrix. The excitation energies of the levels and their population, suggestive of yrast or near-yrast character, match well with the expected cascade of $E2$ transitions between seniority $\nu = 5$ states associated with an $(h_{11/2})^4 d_{3/2}$ structure. Therefore, the states are tentatively assigned as $I^\pi = (27/2^+)$ 3731 keV, $(31/2^+)$ 4921 keV, and $(35/2^+)$ 5311 keV. Also, the observed, relatively strong, feeding of the 6199-keV level suggests its likely yrast nature and a $(39/2^+)$ spin parity is tentatively proposed, defining this state as a $\nu = 7$ excitation (see Sec. IV B).

The prompt transitions and the level scheme above the $27/2^-$ isomer were established based on the delayed coincidence relationships with the four most intense gamma rays associated with its decay at 175, 512, 1105, and 1220 keV. In the (PDD) cube sorted with the delay range optimized for the 39-ns half-life, double (DD) gates were placed on all combinations of these four delayed lines, resulting in coincidence data providing the unambiguous identification of 13 prompt (P) feeding transitions. The sum of such identification spectra from all three measurements is displayed in Fig. 3(e) with the new ^{119}Sn transitions identified. Other lines, corresponding to transitions from the complementary fission fragments, are present as well. The construction of the level scheme above the long-lived $27/2^-$ state could then proceed, based on (PP) matrices derived from the (PPD) cubes with delayed (D) coincidence gates placed on the four intense lines mentioned above. In the earlier study of Astier *et al.* [11] only the three most intense gamma rays (1179, 877, and 828 keV) were identified above the $27/2^-$ isomer. The complexity of the structure established here is consistent with expectations for seniority $\nu = 5$ states in this relatively light isotope. Regarding spin-parity assignments, the general assumption of negative parity for all of the new states seemed justified and is also supported by the absence of any connection with the positive-parity levels built on the $23/2^+$ isomer. While $(31/2^-)$ and $(35/2^-)$ yrast states should be expected from the $\nu(h_{11/2})^5$ structure, several other negative-parity levels may arise from the $\nu(h_{11/2})^3$ configuration coupled to two neutron holes occupying any of the other available, positive-parity single-particle levels. The noteworthy branching observed in the decay from the 5110-keV level suggests an $M1$ character for most of the competing transitions: at least for the lowest-energy 201-, 294-, and 320-keV branches, the alternative $E2$ multipolarity appears unlikely. Consequently, with these decays followed by high-energy $E2$ transitions connecting it to the $27/2^-$ isomer, the 5110-keV yrast level was assigned tentatively as $(33/2^-)$. The intermediate levels at 4282, 4789, 4816, and 4909 keV are proposed as $I^\pi = (31/2^-)$, with the strongly populated 4282-keV state clearly being yrast. Also, the intense population of the 5460-keV level above the 5110-keV, $(33/2^-)$ state argues for its yrast character and allows for its assignment as the expected $(35/2^-)$ highest-spin excitation of $\nu = 5$ seniority. Finally, a $(29/2^-)$ assignment, rather than the $(31/2^-)$ alternative, is preferred for the strongly populated level at 3979 keV. The energy of the 877-keV transition appears to be too low to correspond to an $E2$ transition above the $27/2^-$ isomer, and the yrast population and feeding from above fit well with the $(29/2^-)$ assignment. Three gamma transitions, apparently all of $M1$ multipolarity, populate this level from the $(31/2^-)$ states assigned above and the weak 1130-keV transition from the $(33/2^-)$ level is compatible with it being an $E2$ transition competing with the $M1$ decays from the 5110-keV level (see above). All of these assignments satisfy numerous internal consistency checks within the level scheme of Fig. 2. Yet, they remain tentative in the absence of direct experimental information.

B. ^{121}Sn

The $19/2^+$ and $27/2^-$ isomers in ^{121}Sn were established in Refs. [18] and [6] as decaying through a sequence of gamma rays to the 6-keV, $11/2^-$ long-lived ($T_{1/2} = 49$ y) isomer with respective 5.3-μs and 167-ns half-lives. In the course of the present study, the experimental information on ^{121}Sn was significantly expanded, although a sizable fraction of the new findings has already been reported by Astier *et al.* [11]. Hence, the present discussion can be viewed as an independent confirmation of the results reported in Ref. [11], with an emphasis placed both on differences between the two works and on newly observed levels and transitions. Among the latter, a significant contribution relates to an extension of the experimental information available below the $27/2^-$ isomer. The results are summarized in the level scheme of Fig. 4, the coincidence spectra of Fig. 5 documenting important features, and the list of ^{121}Sn transition energies and intensities of Table II.

In the lowest part of the level scheme, the gamma branching in the decay of the $19/2^+$ isomer has now been determined accurately from the intensities of the 752- and 841-keV transitions listed in Table II. The main decay from the $27/2^-$ isomer proceeds through a cascade of four intense transitions, but a weak branch of coincident 202- and 1298-keV gamma rays was observed between the $23/2^-$ and $15/2^-$ levels. Both transitions must be of $E2$ character and the new state at 2455 keV can be uniquely established as a second $19/2^-$ level. The existence of the 2221-keV, $23/2^+$ isomeric state, reported tentatively by Astier *et al.* [11], was confirmed and its half-life was measured to be $T_{1/2} = 0.52(5)$ μs, in agreement with the value that had been estimated in the previous work. Here, the suggested $23/2^+$ assignment was verified through the observation of new transitions populating this state in the $27/2^-$ isomeric decay. The spectrum displayed in Fig. 5(a) was obtained from the (ddD) cube by placing a gate on the 223-keV transition with long delay (D) below the $23/2^+$ isomer and a (d) gate on the 176-keV line initiating the $27/2^-$ isomer decay. The three delayed (d) lines seen in this spectrum represent the new gamma rays linking the $23/2^-$ level with the $23/2^+$

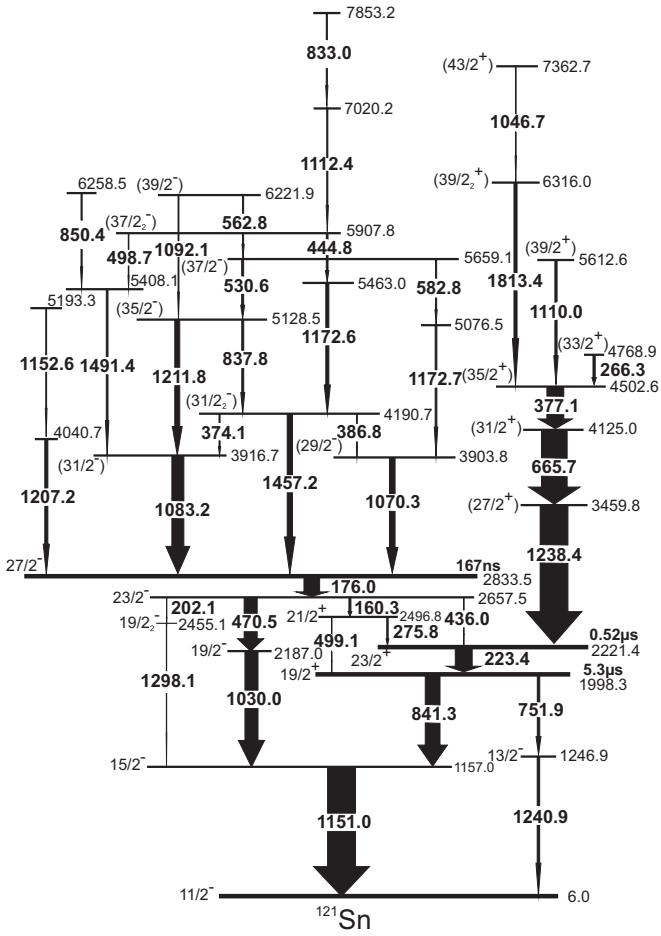

FIG. 4. The ^{121}Sn level scheme established in the present study. The arrow widths reflect the observed intensities in prompt and delayed transitions normalized separately. The spin-parity assignments are discussed in the text.

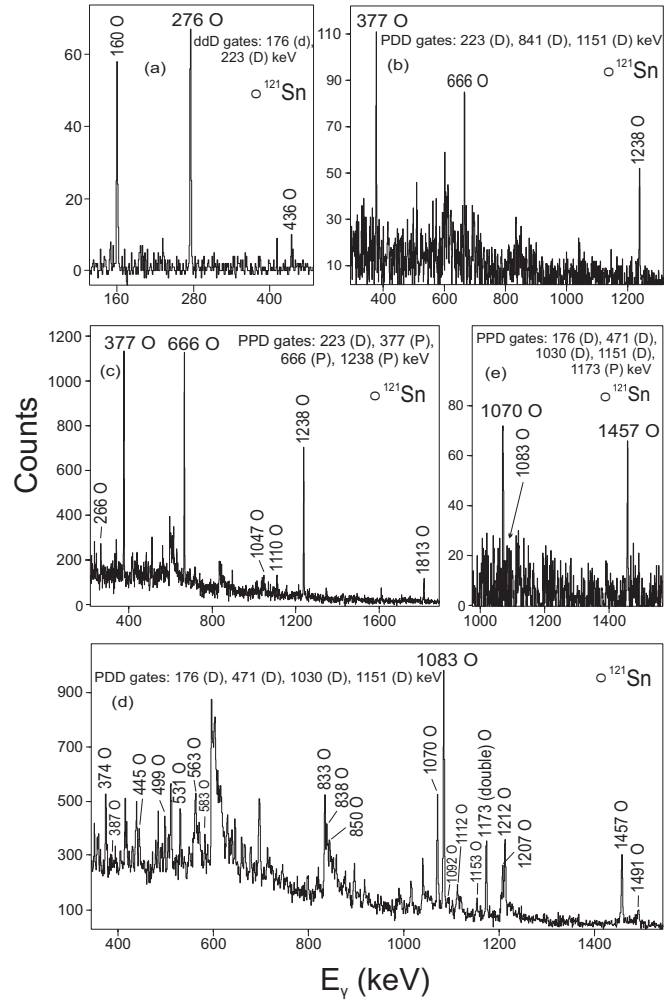

FIG. 5. Important coincidence spectra instrumental in the extension of the ^{121}Sn level scheme. The delayed spectrum (a) documents the decay of the $23/2^-$ level to the $23/2^+$ isomeric state. Other panels include spectra of prompt transitions located above the $23/2^+$ level (b) and (c), and above the $27/2^-$ isomer (d) and (e). The detailed description of the gating conditions and the conclusions drawn from the observed spectra can be found in the text.

long-lived state via the 160-276-keV cascade and a 436-keV cross-over transition. Moreover, in the spectrum obtained with the double gate placed on the 176- and 160-keV gamma rays in the (DDD) cube (not shown), apart from the intense 276-keV line, the 499-keV transition is observed and identified as a parallel decay branch from the new 2497-keV state to the $19/2^+$ isomer. In this part of the level scheme of Fig. 4, the level sequence is analogous to that discussed earlier for ^{119}Sn. Consequently, the same arguments provide spin-parity assignments of $23/2^+$ and $21/2^+$ to the new levels at 2221 and 2497 keV, respectively.

The three prompt transitions at 377, 666, and 1238 keV, seen in the coincidence spectrum of Fig. 5(b), were firmly identified as preceding in time the $23/2^+$ isomer by placing the delayed (D) double gates on transitions below this long-lived state in the (PDD) cube. A more extended structure can be observed in the sum spectrum selected from the (PPD) data with gates on the delayed (D) 223-keV line and the three prompt (P) gamma rays identified above: See Fig. 5(c), where four additional, weaker transitions of 266, 1047, 1110, and 1813 keV are visible together with the stronger sequence of Fig. 5(b). The available coincidence relationships resulted in the level structure proposed in Fig. 4. An almost identical sequence was established by Astier *et al.* [11] and, apart from the confirmation of this part of the level scheme, the present results identify one new 266-keV line feeding the 4503-keV level and verify the existence of the 1047-keV transition (see Fig. 4) which had been proposed as tentative earlier. The $(27/2^+)$, $(31/2^+)$, and $(35/2^+)$ spin-parity assignments to the strongly populated 3460-, 4125-, and 4503-keV levels define the expected sequence of seniority $\nu = 5$ states observed already in ^{119}Sn and agree with the I^π values of Ref. [11]. The tentative $(39/2^+)$ assignment to the 6316-keV level is suggested based on the likely $E2$ character of the 1813-keV transition. The latter is based on the observation that this line does not exhibit any Doppler broadening in the coincidence spectra, indicating a state lifetime longer than 1 ps. A similar argument may hold for the 5613- and 7363-keV levels, however, the lower energy of the 1110- and 1047-keV

TABLE II. Same as Table I, but for ^{121}Sn. The intensities of delayed gamma rays are normalized to the 1151-keV line while for the prompt lines, marked with an asterisk, the normalization refers to the 1238-keV transition.

E_{level} (keV)	I^{π}	E_{γ} (keV)	I_{γ}
6.0	$11/2^{-}$		
1157.0	$15/2^{-}$	1151.0(1)	100
1246.9	$13/2^{-}$	1240.9(2)	9(2)
1998.3	$19/2^{+}$	751.9(2)	9(2)
		841.3(1)	53(5)
2187.0	$19/2^{-}$	1030.0(1)	47(4)
2221.4	$23/2^{+}$	223.4(2)	60(5)
2455.1	$19/2_2^{-}$	1298.1(4)	1.0(4)
2496.8	$21/2^{+}$	275.8(2)	5(1)
		499.1(4)	2.0(7)
2657.5	$23/2^{-}$	160.3(2)	7(2)
		202.1(4)	1.0(4)
		436.0(3)	1.0(4)
		470.5(1)	47(4)
2833.5	$27/2^{-}$	176.0(1)	56(5)
3459.8	$(27/2^{+})$	1238.4(2)	100*
3903.8	$(29/2^{-})$	1070.3(1)	20(3)*
3916.7	$(31/2^{-})$	1083.2(1)	43(3) *
4040.7		1207.2(2)	11(2)*
4125.0	$(31/2^{+})$	665.7(2)	92(8)*
4190.7	$(31/2_2^{-})$	374.1(3)	4(1)*
		386.8(5)	2(1)*
		1457.2(1)	19(3)*
4502.6	$(35/2^{+})$	377.1(2)	60(5)*
4768.9	$(33/2^{+})$	266.3(3)	8(2)*
5076.5		1172.7(1)	6(1)*
5128.5	$(35/2^{-})$	837.8(3)	7(2)*
		1211.8(1)	18(3)*
5193.3		1152.6(3)	3.0(5)*
5408.1		1491.4(2)	6(1)*
5463.0		1172.6(1)	11(2)*
5612.6	$(39/2^{+})$	1110.0(3)	8(2)*
5659.1	$(37/2^{-})$	530.6(1)	7(1)*
		582.8(3)	4(1)*
5907.8	$(37/2_2^{-})$	444.8(2)	6(1)*
		498.7(4)	2.0(5)*
6221.9	$(39/2^{-})$	562.8(3)	4(1)*
		1092.1(3)	3.0(5)*
6258.5		850.4(3)	4(1)*
6316.0	$(39/2_2^{+})$	1813.4(3)	10(2)*
7020.2		1112.4(3)	4(1)*
7362.7	$(43/2^{+})$	1046.7(4)	2.0(7)*
7853.2		833.0(4)	4(1)*

depopulating transitions does not exclude the possibility of a lower multipolarity. Finally, the 4769-keV state is clearly nonyrast and is, tentatively, assigned as a $(33/2^{+})$ level that will be addressed in the discussion section.

The fairly complex spectrum displayed in Fig. 5(d) served to identify prompt (P) transitions above the $27/2^{-}$ isomer selected from the (PDD) cube by placing delayed (DD) double gates on all pairs among the four strongest lines seen in the isomeric decay. The relevant energies and intensities are listed in Table II. The subsequent (PP) coincidence analysis, which used the matrix selected from the (PPD) cube by placing gates on the same four delayed (D) gamma rays, established a fairly elaborate level structure above the $27/2^{-}$ isomer (see Fig. 4). While the placement of the six most intense transitions confirmed the level scheme reported in Ref. [11], the present results established the placement of 15 additional transitions and led to some rearrangements and differences with respect to the earlier work. Two transitions of 889 and 1152 keV are reported in Ref. [11] as bypassing the $27/2^{-}$ isomer. The former was not observed in the present data, while the latter is now placed above the 1207-keV gamma ray feeding the 27/2- isomer. On the other hand, the 1173-keV transition, placed in Ref. [11] directly above the 1070-keV line, has now been established to be an unresolved doublet where the two components are part of parallel sequences. The most intense part of this doublet feeds the 4191-keV level which is depopulated mostly through a 1457-keV transition. This new placement is documented in Fig. 5(e), where transitions in coincidence with the 1173-keV doublet are displayed. Both the 1070- and 1457-keV lines are present and these are firmly placed in parallel in the scheme of Fig. 4. Here, the presence of the intense 1070-keV line cannot be explained by a weak 387-keV transition connecting the 4191- and 3904-keV levels because the 1083-keV gamma ray from the 3917-keV state connected via the even stronger 374-keV branch is barely visible, as indicated in Fig. 5(e). Note that established coincidence relationships in the higher part of the level scheme also verify the existence of the unresolved 1173-keV doublet.

Although, as was the case in ^{119}Sn, the observed ^{121}Sn structure above the $27/2^{-}$ isomer likely involves only negative-parity levels; the spin-parity assignments to most states are based on somewhat speculative arguments and, hence, are tentative. The yrast and near-yrast population, the observed deexcitation patterns, and the systematics of level energies over the entire Sn isotopic chain are the main arguments taken into consideration. In a number of cases, the results of shell-model calculations provided additional support. Nevertheless, the $(31/2^{-})$ and $(35/2^{-})$ assignments to the 3917- and 5129-keV levels appear to be rather certain: These states stand out by their strong yrast population and by excitation energies that are more than 300 keV lower than the corresponding levels in ^{119}Sn, as expected from the variations with mass A discussed below. Also, the $(31/2^{-})$ spin parity of the 4191-keV level reflects its near-yrast status, while the 3904-keV state fits well with the $(29/2^{-})$ assignment of a similar yrast state seen in ^{119}Sn. In a more speculative way, the deexcitation patterns from the 5659- and 5908-keV levels are in line with the suggested $(37/2^{-})$ assignments. Note that this $(37/2^{-})$ assignment for the 5659-keV level is also the highest possible one for this state when starting from $I^{\pi} = (29/2^{-})$ for the 3904-keV state. Following similar considerations leads to $I^{\pi} = (39/2^{-})$ for the 6222-keV level with the 1092-keV, $E2$ branch to the $(35/2^{-})$ state competing with the 563-keV $M1$ transition to the 5659-keV, $(37/2^{-})$ one. It should be kept in mind that the ^{121}Sn level scheme extends to nearly 8-MeV excitation energy with highest-spin states around $41/2$ or $43/2$, and all levels above spin $35/2$ likely corresponding to seniority $\nu = 7$ excitations. The latter are, at present, rather difficult to

calculate with an accuracy suitable for conclusive support of tentative experimental assignments.

C. ^{123}Sn

Results of the present study for the ^{123}Sn isotope are summarized in the level scheme of Fig. 6 and in Table III. The level scheme is in full agreement with earlier results presented in Refs. [6,18] which focused on the decay of three isomeric states with respective lifetimes and spin-parity quantum numbers of 7.4 μs $19/2^+$, 6 μs $23/2^+$, and 34 μs $27/2^-$. Above these isomers, associated with seniority $\nu = 3$ excitations, higher-seniority states were reported in Ref. [11]. Here as well, the present results largely confirm the proposed level scheme. However, a few noteworthy features have been established both above and below the long-lived states. Spectra emphasizing these new findings are displayed in Fig. 7. In the upper panel [Fig. 7(a)], a coincidence spectrum obtained from the (DDD) cube by placing delayed double gates on the 170-

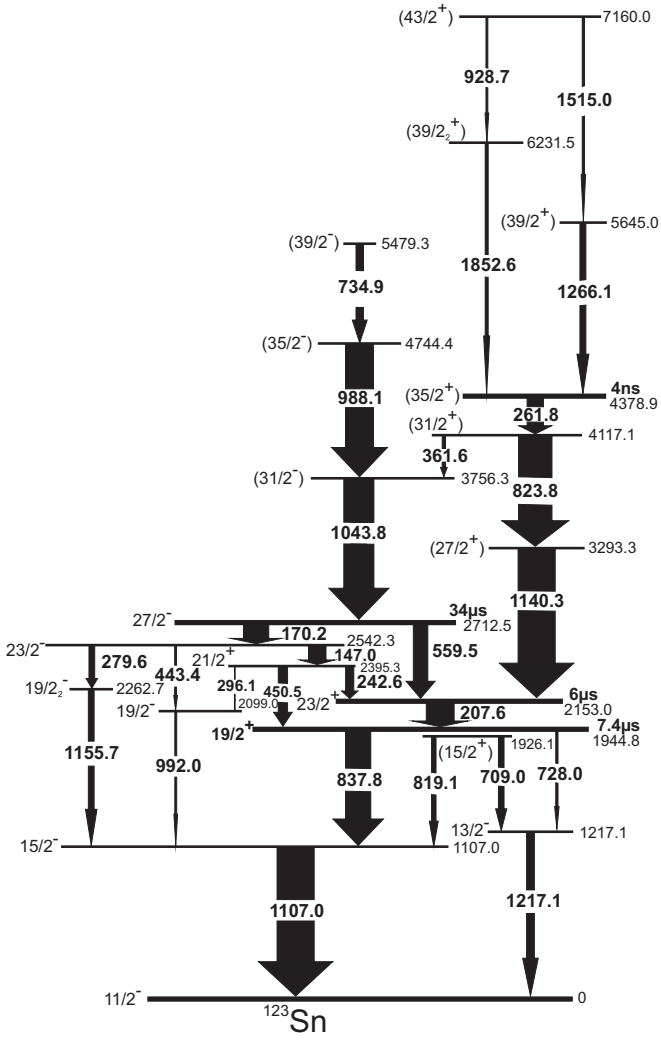

FIG. 6. The ^{123}Sn level scheme established in the present study. The arrow widths reflect the observed intensities in prompt and delayed transitions normalized separately. The spin-parity assignments are discussed in the text.

TABLE III. Same as Table I, but for ^{123}Sn. The intensities of delayed gamma rays are normalized to the 1107-keV line while for prompt gamma rays, marked with an asterisk, the normalization is to the 1140-keV transition.

E_{level} (keV)	I^π	E_γ (keV)	I_γ
0.0	$11/2^-$		
1107.0	$15/2^-$	1107.0(1)	100
1217.1	$13/2^-$	1217.1(1)	21(2)
1926.1	$(15/2^+)$	709.0(1)	15(2)
		819.1(2)	12(2)
1944.8	$19/2^+$	18.7[a]	0.02[a]
		728.0(2)	6(1)
		837.8(1)	67(5)
2099.0	$19/2^-$	992.0(2)	5(1)
2153.0	$23/2^+$	207.6(2)	75(7)
2262.7	$19/2_2^-$	1155.7(2)	16(2)
2395.3	$21/2^+$	242.6(2)	22(2)
		296.1(5)	2.0(8)
		450.5(2)	25(2)
2542.3	$23/2^-$	147.0(2)	47(5)
		279.6(2)	16(2)
		443.4(2)	5(1)
2712.5	$27/2^-$	170.2(1)	68(6)
		559.5[b]	47[b]
3293.3	$(27/2^+)$	1140.3(2)	100*
3756.3	$(31/2^-)$	1043.8(3)	81(7)*
4117.1	$(31/2^+)$	361.6(5)	9(4)*
		823.8(2)	90(8)*
4378.9	$(35/2^+)$	261.8(2)	44(5)*
4744.4	$(35/2^-)$	988.1(3)	75(7)*
5479.3	$(39/2^-)$	734.9(4)	20(2)*
5645.0	$(39/2^+)$	1266.1(3)	16(2)*
6231.5	$(39/2_2^+)$	1852.6(3)	8(2)*
7160.0	$(43/2^+)$	928.7(3)	5(1)*
		1515.0(3)	6(1)*

[a]Unobserved. The intensity was calculated using the summed intensities of the 709- and 819-keV lines and with an electron-conversion coefficient for an $E2$ multipolarity.

[b]The 560-keV $M2$ transition could not be observed in the present study; the intensity was deduced from the $B(E2)$ value extracted for the 170-keV isomeric transition in the $27/2^-$ decay study of Ref. [6].

and 1107-keV gamma rays provides evidence not only for the intense 280- and 1156-keV transitions reported earlier, but also for two new lines of 443 and 992 keV.

Analysis of other coincidence relationships confirmed that this establishes an additional decay branch in the decay of the 34-μs isomer resulting in a new, $19/2^-$ yrast level at 2099 keV. The coincidence spectrum of Fig. 7(b), with delayed gates placed on the 992- and 1107-keV lines, also reveals a weak, 296-keV gamma ray. The latter line was also seen in other coincidence spectra justifying its placement as a link between the 2395-keV, $21/2^+$ level and the new $19/2^-$ state. The existence of this decay branch also solidifies the $21/2^+$ assignment to the 2395-keV level. In Fig. 7(b), the weak trace of a 280-keV line is indicated together with the position of an expected 164-keV gamma ray that would correspond to a possible $M1$ connection between the two $19/2^-$ states.

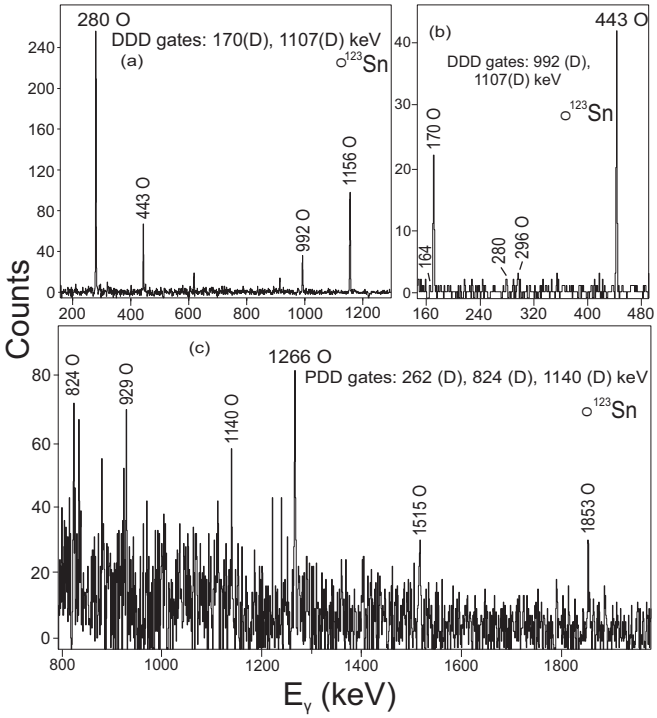

FIG. 7. Coincidence spectra relevant for the ^{123}Sn level scheme. The delayed spectra (a) and (b) document the decay of the $27/2^-$ isomer. (b) The position of the 164-keV line is indicated as it would represent the link between the 992-keV gating transition and the 280-keV gamma ray observed weakly in the spectrum (see text for details). The prompt spectrum (c) was obtained with the delayed double coincidence gates placed on the three gamma rays in the decay of the short-lived $(35/2^+)$ isomer.

However, this evidence was deemed to be inconclusive. In the lower part of the scheme, a $(15/2^+)$ assignment was adopted for the 1926-keV level following results and systematics presented by Pinston *et al.* [20]. Note that none of the previous publications provided the intensities of gamma branches associated with the decay of the $19/2^+$ isomer decay; the relevant data are listed here in Table III.

The level scheme established above the $23/2^+$ isomer (Fig. 6) fully confirmed the results reported by Astier *et al.* [11], and more precise energy and intensity values are provided here (Table III). Also, tentative spin-parity assignments were adopted following the same approach as above. These assignments extend to the highest-spin states observed and use was made, for example, of the likely $E2$ character of high-energy transitions, based on the absence of Doppler broadening indicating state lifetimes longer than 1 ps. A significant new result of the present work is the determination of a $T_{1/2} = 4(1)$ ns half-life for the $(35/2^+)$ state at 4379 keV. Although the determination of this short half-life required special care, the spectrum of Fig. 7(c) demonstrates existence of the isomer. In this instance, the (PDD) cube was sorted while requiring a short 3- to 30-ns delay range and the delayed gates were placed on every possible combination of the three strong transitions in the sequence below the $(35/2^+)$ isomer. While this selected range includes contributions from prompt gamma rays, because of the relatively poor timing of large Ge detectors, the strong enhancement of (P) transitions above the isomer and the notable reduction of (D) lines below the $(35/2^+)$ level is, nevertheless, clearly visible in the spectrum, herewith confirming the presence of the long-lived state. Thus, it appears that the half-filling of the $h_{11/2}$ subshell, which manifests itself through transitions between states of $(h_{11/2})^n$ character with the lowest $B(E2)$ values in the Sn isotopic chain, is also reflected in the properties of this $(35/2^+)$ state.

The standard delayed-coincidence technique could not be used to identify transitions preceding the $27/2^-$ isomer because of the long, 34-μs half-life. The complex analysis with the cross-coincidence method described in Ref. [10] could only locate tentatively a 1044-988-735-keV cascade in ^{123}Sn. Also, in a similar analysis, Astier *et al.* [11] assigned tentatively two cascades of three transitions each, both above the $27/2^-$ isomer. Their second cascade, consisting of 1107-, 992-, 710-keV transitions was not observed in the present work, and the first two gamma rays involved also appear in the lower part of the level scheme, leading one to question the proposed, tentative assignment. The conclusive argument in favor of placing the 1044-988-735-keV cascade as proposed in Fig. 6, and establishing the yrast $(31/2^-)$ 3756-keV, $(35/2^-)$ 4744-keV, and $(39/2^-)$ 5479-keV levels, comes from the observation of the 362-keV transition feeding the lowest $(31/2^-)$ level from the $(31/2^+)$, 4117-keV state. In lighter Sn isotopes, such a connection between the positive- and negative-parity states above the $23/2^+$ and $27/2^-$ isomers, respectively, could not be observed. Here, in ^{123}Sn, the 362-keV $E1$ gamma ray is seen to compete with the 824-keV $E2$ transition because of the expected low $B(E2)$ transition probability of the latter one (see above). Finally, it should be noted that, as in lighter isotopes, many other negative-parity levels should be expected above the $27/2^-$ isomer in ^{123}Sn. However, in the present experiments, their identification was not possible, most likely because the reaction mechanisms favor feeding of yrast states; i.e., of the levels with positive parity.

D. ^{125}Sn

In a series of earlier studies, a rather complete level scheme was established below the $27/2^-$ isomer in ^{125}Sn. The decay of this 0.23-μs state via cascades of four $E2$ transitions, with separate branches populating two $19/2^-$ levels, was reported in Ref. [7]. A more detailed study of this decay, described in Ref. [19], revealed a connection between the $27/2^-$ and $19/2^+$ isomers and identified the $23/2^+$ long-lived state with a 0.6(1)-μs half-life. Moreover, within the systematic study of the deexcitation of $19/2^+$ isomers in the isotopic chain [19], the 6.2(7)-μs half-life was reported for this level in ^{125}Sn with an intense $E2$ decay branch populating the $15/2^+$ level. In this part of the level scheme, little information was added in the present study, for which the results are summarized in the level scheme of Fig. 8 and the transition energies and intensities of Table IV.

The intensities of the gamma rays involved in the $19/2^+$ isomeric decay were determined and the values listed in Table IV confirm the results of Ref. [19]. An additional weak

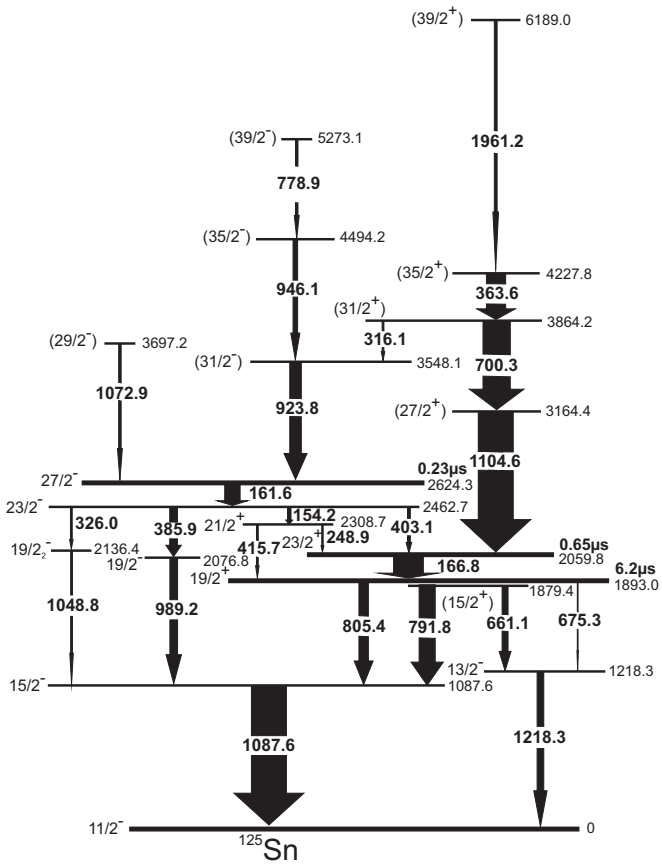

FIG. 8. The ^{125}Sn level scheme established in the present study. The arrow widths reflect the observed intensities in prompt and delayed transitions normalized separately. The spin-parity assignments are discussed in the text.

TABLE IV. Same as Table I, but for ^{125}Sn. The intensities of delayed gamma rays are normalized to the 1088-keV line while prompt gamma rays, marked with an asterisk, are normalized to the 1105-keV transition.

E_{level} (keV)	I^{π}	E_{γ} (keV)	I_{γ}
0.0	$11/2^{-}$		
1087.6	$15/2^{-}$	1087.6(1)	100
1218.3	$13/2^{-}$	1218.3(1)	19(2)
1879.4	$(15/2^{+})$	661.1(1)	21(2)
		791.8(1)	46(4)
1893.0	$19/2^{+}$	13.6[a]	0.01[a]
		675.3(4)	2.0(7)
		805.4(1)	33(2)
2059.8	$23/2^{+}$	166.8(2)	85(8)
2076.8	$19/2^{-}$	989.2(1)	22(2)
2136.4	$19/2^{-}_{2}$	1048.8(2)	5(1)
2308.7	$21/2^{+}$	248.9(2)	4(1)
		415.7(3)	5(1)
2462.7	$23/2^{-}$	154.2(2)	9(2)
		326.0(2)	5(1)
		385.9(1)	22(2)
		403.1(2)	8(2)
2624.3	$27/2^{-}$	161.6(1)	44(4)
3164.4	$(27/2^{+})$	1104.6(2)	100*
3548.1	$(31/2^{-})$	923.8(2)	33(3)*
3697.2	$(29/2^{-})$	1072.9(2)	7(1)*
3864.2	$(31/2^{+})$	316.1(2)	5(1)*
		700.3(2)	78(7)*
4227.8	$(35/2^{+})$	363.6(2)	55(5)*
4494.2	$(35/2^{-})$	946.1(2)	13(2)*
5273.1	$(39/2^{-})$	778.9(3)	7(1)*
6189.0	$(39/2^{+})$	1961.2(4)	8(2)*

[a]Unobserved. The intensity was calculated using the summed intensities of the 661- and 792-keV transitions and an electron conversion coefficient assuming an $E2$ multipolarity.

$E3$ branch, through a 675-keV line, was observed; this was also the case in ^{123}Sn. The half-life of the $23/2^{+}$ isomer was measured to be 0.65(6) μs, in good agreement with the earlier determination [19]. A new, somewhat intense 249-keV transition was identified as populating the $23/2^{+}$ long-lived state in the $27/2^{-}$ isomeric decay. The evidence is illustrated in the spectrum of Fig. 9(a) obtained from the (ddD) cube by placing gates on the delayed (d) 162-keV line together with the (D) transitions below the $23/2^{+}$ isomer listed in the figure. This observation of the 249-keV line completes the analogy between the isomeric decays of the $27/2^{-}$ levels in ^{125}Sn and in the lighter Sn isotopes and solidifies the $21/2^{+}$ assignment to the 2309-keV level. The absence of the 416-keV transition in Fig. 9(a) indicates that contributions of coincidence events across the 6.2-μs isomer are negligibly small. It is also worth noting that the intensities of the 154- and 416-keV transitions (Table IV) were not reported earlier, while the intensity given here for the 403-keV transition is significantly lower than that found in Ref. [19].

In the upper part of the level scheme in Fig. 8, two cascades were identified as feeding the $23/2^{+}$ and $27/2^{-}$ isomers, respectively. Only the one feeding the $27/2^{-}$ level was reported earlier by Astier *et al.* [11], even though it appears to be populated with about three times lower intensity. Delayed coincidence spectra with a single gate placed on the delayed (D) 167-keV transition in the [PD] matrices, extracted from data sets from all three experiments, revealed the 1105-700-364-keV cascade feeding the $23/2^{+}$ isomer. In the spectrum of Fig. 9(b), obtained from the ^{48}Ca + ^{238}U data, these lines are clearly visible despite the limited selectivity provided by a single coincidence gate and, an additional, weaker fourth transition of 1961 keV can be seen as well. A cleaner spectrum showing these four transitions is displayed in Fig. 9(c). It was obtained from the (PPD) cube by placing the delayed (D) gate on the 167-keV line together with prompt (P) ones on the three strongest lines in the cascade. Additional support verifying the identification of this sequence was provided by the observed link with a negative-parity level located above the $27/2^{-}$ isomer. The prompt coincidence spectrum of Fig. 9(d) was obtained from the (PDD) cube by placing double delayed (D) gates on all the combinations among the four most intense gamma rays in the $27/2^{-}$ isomeric decay. The transitions feeding this long-lived state are all visible and, apart from the 924-946-779-keV cascade reported in Ref. [11] and confirmed here, three less intense lines of 316, 364, and 1073 keV

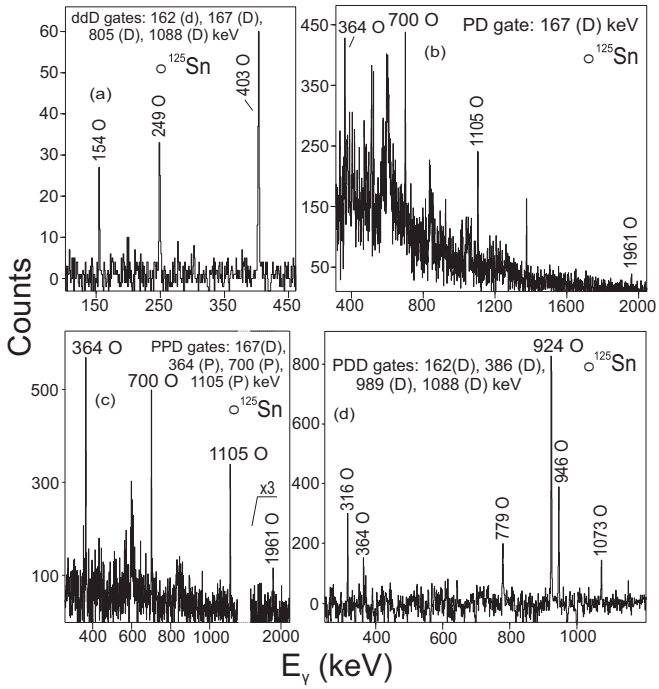

FIG. 9. Crucial coincidence spectra used to establish the ^{125}Sn level scheme. The delayed spectrum (a) documents the feeding of the $23/2^+$ isomer from the $27/2^-$ isomeric decay. In other panels, spectra of prompt transitions above the $23/2^+$ (b) and (c), and $27/2^-$ (d) isomers are shown. See text for a detailed description of the gating conditions and for the conclusions drawn from the observations.

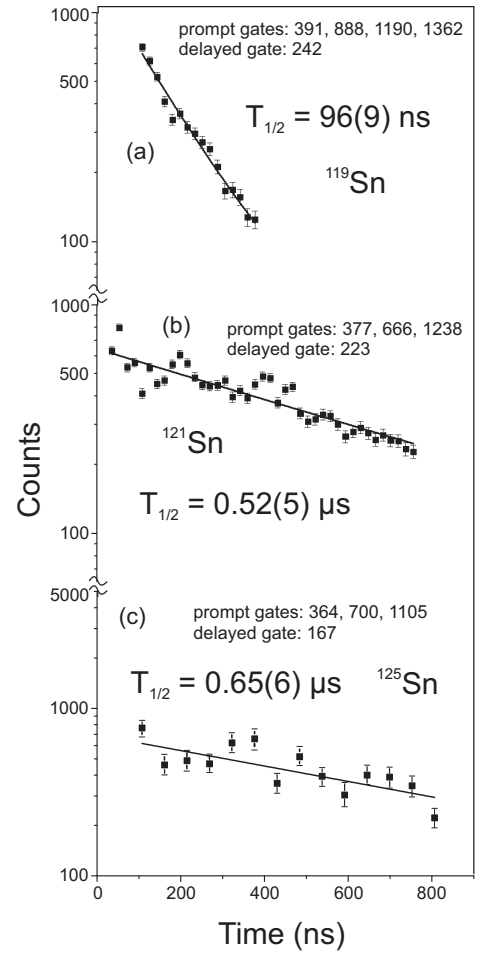

FIG. 10. Time distributions used to determine the half-lives of the $23/2^+$ isomers in ^{119}Sn (a), ^{121}Sn (b), and ^{125}Sn (c). The time spectra were obtained by placing gates on the three most intense gamma rays above the isomers and a specific delayed isomeric transition (see text for details). The half-lives and uncertainties take into account variations associated with changes in the gating conditions.

can be observed. The coincidence analysis established the simple structure of high-spin, negative-parity states proposed in Fig. 8. As already alluded to above, one of the crucial elements in the construction of this part of the level scheme was the placement of the 316-keV link with the positive-parity states which also accounts for the presence of the 364-keV line in Fig. 9(d). The three strongest transitions define the anticipated sequence of $(31/2^-)$, $(35/2^-)$, and $(39/2^-)$ yrast levels. The 1073-keV gamma ray was not in coincidence with any other transition above the $27/2^-$ isomer and was placed as feeding it directly from a level tentatively assigned as $(29/2^-)$ on the basis of the analogy with similar states in lighter Sn isotopes. The positive-parity levels above the $23/2^+$ isomer are associated with the $(27/2^+)$, $(31/2^+)$, and $(35/2^+)$ yrast sequence observed also in the other isotopes. Finally, the highest-energy 6189-keV stated is suggested to correspond to a $(39/2^+)$ level, based on the lifetime considerations related to the narrowness of the 1961-keV line.

E. Half-life determinations and transition probabilities

Three isomeric states with spin parity $I^\pi = 19/2^+, 23/2^+$, and $27/2^-$ were observed in each of the Sn isotopes under investigation and a fourth, shorter-lived $(35/2^+)$ level was identified in ^{123}Sn only. Most of these isomers are known from earlier studies [6,18–20] and, in many instances, the reported half-lives were adopted in the present work. Figure 10 provides the decay curves used here to determine the half-lives of the $23/2^+$ isomers in ^{119,121}Sn and ^{125}Sn. In ^{119}Sn, the $23/2^+$ isomer was not known prior to this work. In ^{121}Sn, on the other hand, it had been identified [11], but the half-life had only been estimated from a reduction in the intensity of the isomeric transition in coincidence spectra. For the $23/2^+$ isomer in ^{125}Sn, Ref. [19] reported a half-life with a somewhat large uncertainty [0.6(2) μs] that took into account a possible contribution by feeding from the higher-lying 0.23-μs state. Hence, the present half-life determination for this $23/2^+$ level confirms the earlier value and improves on its accuracy. Also, the half-life of the $27/2^-$ long-lived state in ^{119}Sn was confirmed and a more precise value of 39(3) ns was measured.

The relevant decay curves were obtained as time distributions between the strong gamma rays feeding the $23/2^+$ isomers and those associated directly with their decay: The relevant transition energies are indicated in the various panels of Fig. 10. The 96(9)-ns, 0.52(5)-μs, and 0.65(6)-μs half-lives

TABLE V. The reduced transition probabilities observed in the decay of isomeric states in the odd $^{117-129}$Sn isotopes (see text for details). The corresponding $B(E\lambda)$ and $B(M\lambda)$ values are provided in (e^2fm$^{2\lambda}$) and in (μ_N^2fm$^{2\lambda-2}$), respectively, as well as in Weisskopf units. The transition energies, half-lives, and branching are given in columns 2, 4, and 5, respectively.

	E_γ(keV)	$I_i \rightarrow I_f$	$T_{1/2}$ (μs)	Branching (%)	$B(E\lambda)$ (e^{2}fm$^{2\lambda}$) $B(M2)$ (μ_N^2fm^2)	$B(E\lambda)$, $B(M2)$ (W.u.)
^{117}Sn[a]	5.7[b]	$19/2^+ \rightarrow 17/2^-$, $E1$	1.75(7)	0.70(8)	$1.0(2)\times10^{-5}$	$2.9(5)\times10^{-7}$
	25.4[b]	$19/2^+ \rightarrow (15/2^+)$, $(E2)$		0.059(16)	18(5)	0.53(15)
	813.4	$19/2^+ \rightarrow 15/2^-$, $M2$		19.4(32)	$1.6(3)\times10^{-2}$	$4.0(8)\times10^{-4}$
	781.0	$19/2^+ \rightarrow 13/2^-$, $E3$		2.2(11)	85(43)	0.10(5)
^{119}Sn	174.7	$27/2^- \rightarrow 23/2^-$, $E2$	0.039(3)	81.8(73)	73(7)	2.1(2)
	241.7	$23/2^+ \rightarrow 19/2^+$, $E2$	0.096(9)	93.2(75)	6.7(8)	0.19(2)
	817.7	$19/2^+ \rightarrow 15/2^-$, $M2$	9.6(12)[c]	84.9(75)	$1.2(2)\times10^{-2}$	$3.0(5)\times10^{-4}$
	748.3	$19/2^+ \rightarrow 13/2^-$, $E3$		15.1(19)	147(26)	0.17(3)
^{121}Sn	223.4	$23/2^+ \rightarrow 19/2^+$, $E2$	0.52(5)	91.3(76)	1.8(2)	$5.0(6)\times10^{-2}$
	841.3	$19/2^+ \rightarrow 15/2^-$, $M2$	5.3(5)[c]	85.5(81)	$2.0(3)\times10^{-2}$	$4.9(7)\times10^{-4}$
	751.9	$19/2^+ \rightarrow 13/2^-$, $E3$		14.5(32)	247(59)	0.28(7)
^{123}Sn	261.8	$(35/2^+) \rightarrow (31/2^+)$, $(E2)$	0.004(1)	94.7(98)	109(29)	3.0(8)
	207.6	$23/2^+ \rightarrow 19/2^+$, $E2$	6[c]	89.1(83)	0.22(3)	$6.0(8)\times10^{-3}$
	18.7[b]	$19/2^+ \rightarrow (15/2^+)$, $(E2)$	7.4(26)[c]	0.020(3)	6.7(25)	0.18(7)
	837.8	$19/2^+ \rightarrow 15/2^-$, $M2$		67.0(50)	$1.1(4)\times10^{-2}$	$2.7(10)\times10^{-4}$
	728.0	$19/2^+ \rightarrow 13/2^-$, $E3$		6.0(10)	92(36)	0.10(4)
^{125}Sn	166.8	$23/2^+ \rightarrow 19/2^+$, $E2$	0.65(6)	79.2(75)	5.4(7)	0.15(2)
	13.6[b]	$19/2^+ \rightarrow (15/2^+)$, $(E2)$	6.2(2)[c]	0.012(2)	22(4)	0.6(1)
	805.4	$19/2^+ \rightarrow 15/2^-$, $M2$		32.3(25)	$7.9(7)\times10^{-3}$	$1.87(15)\times10^{-4}$
	675.3	$19/2^+ \rightarrow 13/2^-$, $E3$		1.9(7)	58(21)	$6.2(24)\times10^{-2}$
^{127}Sn[d]	104.3	$23/2^+ \rightarrow 19/2^+$, $E2$	1.2(1)	42.1(13)	16(2)	0.42(5)
	16.4	$19/2^+ \rightarrow (15/2^+)$, $(E2)$	4.5(1)	0.037(8)	39(9)	1.0(2)
	731.8	$19/2^+ \rightarrow 15/2^-$, $M2$		12.5(14)	$6.9(8)\times10^{-3}$	$1.7(2)\times10^{-4}$
^{129}Sn[d]	41.0	$23/2^+ \rightarrow 19/2^+$, $E2$	2.2(1)	2.4(3)	50(10)	1.3(3)
	19.7	$19/2^+ \rightarrow (15/2^+)$, $(E2)$	3.4(4)	0.10(1)	58(9)	1.5(2)

[a]Transition energies and intensities as well as half-lives taken from Ref. [21].
[b]Unobserved. The values inferred from the differences of the level energies.
[c]Half-lives adopted from Refs. [6,18].
[d]Transition energies and intensities as well as half-lives adopted in Ref. [19].

were obtained from fits to the decay curves in Fig. 10(a) for ^{119}Sn, Fig. 10(b) for ^{121}Sn, and in Fig. 10(c) for ^{125}Sn. The present half-lives in ^{121}Sn and ^{125}Sn are in good agreement with previous determinations [11,19].

A short half-life value of 4(1) ns was extracted for the $(35/2^+)$ state in ^{123}Sn from the analysis of the time distribution between transitions populating this level and two high-energy lines associated with the depopulating cascade. The data points were analyzed using both the slope and centroid shift methods. The latter technique takes advantage of direct comparisons with prompt distributions selected by using transitions in other nuclei with energies comparable to those of the lines used as gates in ^{123}Sn. Both methods gave consistent results for the half-life, as noted earlier for cases with similar short-lived isomers in the even Sn isotopes [10].

The reduced probabilities $B(E\lambda)$ for transitions observed in the deexcitation of all known isomers in the odd-Sn isotopes are compiled in Table V. These were extracted from half-lives reported either here or in earlier work, while using mostly information on decay branches from the present study. The $23/2^+$ and $19/2^+$ isomeric $E2$ transitions will be discussed in the next section.

IV. DISCUSSION

A. Systematics of $B(E2)$ transition probabilities

One of the most striking features revealed by the study of the neutron-rich Sn isotopes is the smooth dependence with mass A of the $B(E2)$ reduced transition probabilities of the isomeric transitions. Already for the proton $(h_{11/2})^n$ isomers identified in the $N = 82$ isotones, a regular parabolic dependence of these $B(E2)$ values with Z was observed and interpreted in Ref. [2]. In the Sn isotopes, this phenomenon can be studied in a more complete way over a large mass range, while also including isomers with more complex intrinsic structures.

For the $23/2^+$ and $19/2^+$ isomers in odd-Sn isotopes, the systematics behavior of $B(E2)$ values is presented in Fig. 11 (see also Table V), where it is compared with that established earlier for the 10^+ and $27/2^-$ isomers over the $A = 116$–130 mass range. For isomeric transitions between $\nu(h_{11/2})^n$ states, the dependence of the $B(E2)$ probabilities on the $\nu h_{11/2}$ subshell occupation number n and on the neutron effective charge $e_{\rm eff}$, taking the radial matrix element $\langle r^2\rangle$ for $\nu h_{11/2}$ to be 32 fm^2, can be expressed [22] by the following

equations:

$$B(E2;\ 10^+ \rightarrow\ 8^+) = 1.17(6\text{-}n)^2 e^2_{\rm eff},$$

and

$$B(E2;\ 27/2^- \rightarrow\ 23/2^-) = 4.41(6\text{-}n)^2 e^2_{\rm eff}.$$

Following Refs. [4–8,10], it is convenient to plot the $E2$ transition amplitudes [or square roots of the measured $B(E2)$ values] versus A, using the previously adopted convention that these amplitudes must be of opposite sign in the bottom and top halves of the $\nu h_{11/2}$ subshell, and cross zero at the half-filled shell, when particle and hole contributions cancel each other. Except for the heaviest isotopes, all the $E2$ amplitudes determined for the 10^+ and $27/2^-$ isomers displayed in Fig. 11 follow rather precisely a linear A dependence when the odd-A points are multiplied by 0.514 to compensate for the different geometrical factors entering the $\nu = 2$ and $\nu = 3$ $B(E2)$ equations. In even-Sn isotopes, it was shown in Ref. [10] that the same A dependence is also observed for the seniority $\nu = 4$, 15^-, and 13^- isomers and the 0.514 geometrical reduction factor had to be used to obtain similar amplitude values as for the $\nu = 2$, 10^+ isomers. This reflects the $(h_{11/2})^3 d_{3/2}$ intrinsic structure of these 15^- and 13^- isomers, where the $d_{3/2}$ neutron acts only as a spectator and does not contribute to the $E2$ transition amplitude.

For the $E2$ decay of the short-lived $(35/2^+)$, $\nu = 5$ isomer in ^{123}Sn, the reduced transition probability was calculated as well and the value is included in Table V. This value is much larger than the other $B(E2)$ probabilities found in this isotope. Apparently, the geometrical factors discussed above that result in $E2$ isomeric decays of the $27/2^-$, $\nu = 3$ isomers being faster by nearly a factor 4 than the 10^+, $\nu = 2$ ones can also account for this large $B(E2)$ value. Indeed, this factor will be even larger for the 16^+ coupling of the $(h_{11/2})^4$ configuration involved in the structure of the $35/2^+$ level. This question can be considered in a more quantitative way once the half-lives of the (16^+) states in even-Sn isotopes are measured [at present, the $B(E2)$ value for the $E2$ decay of the $(35/2^+)$ level in ^{123}Sn is the only one available for this configuration].

The $23/2^+$ isomers studied here extend to the $A > 123$ Sn isotopes the systematics of the $23/2^+ \rightarrow 19/2^+$ $E2$ transition probabilities, originally reported by Lozeva *et al.* [19]. The filled squares in Fig. 11 are these amplitudes obtained, for all $23/2^+$ isomers, from the $B(E2)$ values listed in Table V. The $(h_{11/2})^2 d_{3/2}$ structure again involves a $d_{3/2}$ spectator and, as expected in this case, the amplitudes are of the same size as those of the 10^+ isomers. The average slope of the fitted line, calculated to be -0.94 $e\text{fm}^2/A$, is rather close to the -0.83 $e\text{fm}^2/A$ one obtained for the 10^+ and $27/2^-$ isomers and the zero crossing is also observed to lie close to $A = 123$, as expected.

A somewhat less transparent situation occurs in the $E2$ decay of the long-lived $19/2^+$ isomers shown as filled circles in Fig. 11. Pinston *et al.* [20] established the presence of such $19/2^+ \rightarrow 15/2^+$, $E2$ transitions in the ^{125,127,129}Sn isotopes and concluded that an $E2$ branch had to be present in ^{123}Sn as well. This resulted in a $15/2^+$ assignment to the 1926-keV final state rather than the $(17/2^-)$ one proposed tentatively in Ref. [6]. In all these cases, the low-energy $E2$ transitions

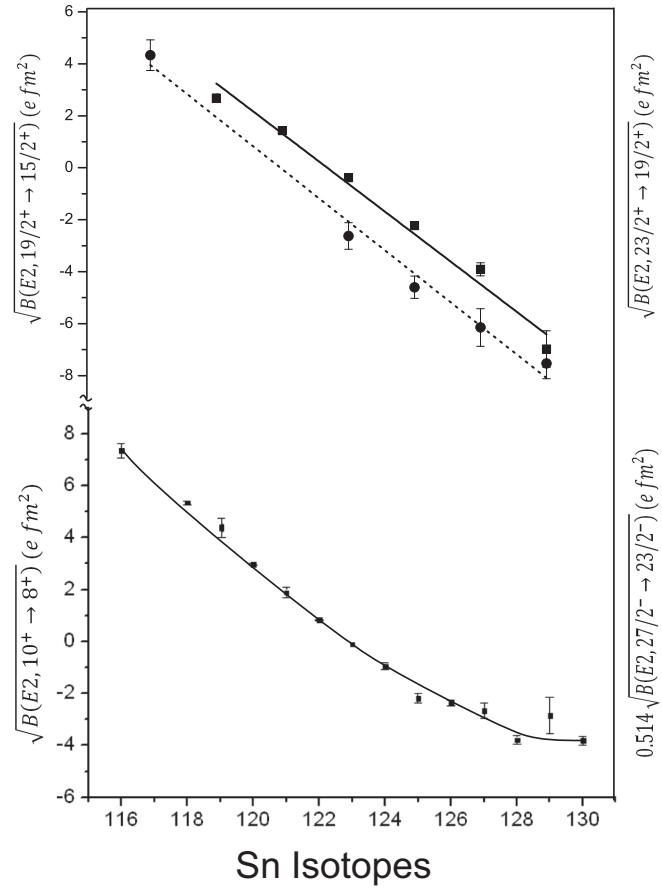

FIG. 11. Amplitudes of the reduced transition probabilities for $E2$ isomeric decays observed in Sn isotopes, calculated from the $B(E2)$ values listed in Table V. In the upper part, the $B(E2)$ amplitudes associated with the $23/2^+$ (squares) and $19/2^+$ (circles) isomeric decays are displayed. These $E2$ transition amplitudes are compared with those determined previously [3–8] for the 10^+ and $27/2^-$ $(h_{11/2})^n$ isomer decays (lower part of the figure). The details are discussed in the text.

could not be detected as they are all below 50 keV, and the extracted $B(E2)$ values used branchings determined from the intensities of gamma rays depopulating the $(15/2^+)$ levels to the lower-lying $13/2^-$ and $15/2^-$ states, as well as the intensities of the $M2$ and $E3$ isomeric decays. In Ref. [20], it was then concluded that the dependence of the $B(E2)$ values follows the trend with A seen for the other isomers, thus reflecting the change in the $h_{11/2}$ subshell occupation. In the present work, these $B(E2)$ values were recalculated with intensities from Ref. [19] for ^{127,129}Sn and from this study for ^{123,125}Sn. Although evidence for similar $19/2^+ \rightarrow (15/2^+)$ $E2$ decays could not be found in the ^{119,121}Sn isotopes, such deexcitation paths may well be present and would have to be discovered in new, dedicated experiments able to overcome the present challenge of identifying very weak branches in long-lived isomeric decays. On the other hand, the ^{117}Sn isotope can be considered here as the $19/2^+$ isomer was identified in the detailed study by Hashimoto *et al.* [21]. In this isomeric decay, apart from the usual $M2$ and $E3$ direct deexcitations seen in a number of other odd-Sn isotope,

evidence for two low-energy 6- and 25-keV transitions was found and these were proposed to populate levels assigned as two $(17/2^-)$ states (see Ref. [21] for details). While the measured electron conversion and angular distributions provide strong evidence for the $17/2^-$ assignment to the 2401-keV level populated by the 6-keV transition, the 25-keV branch could well be the sought-after $E2$ transition populating, with much smaller intensity, the $15/2^+$ level at 2381 keV. Since no evidence was presented for the $17/2^-$ assignment in Ref. [21], the $(15/2^+)$ spin parity was adopted here and the extracted $B(E2)$ value resulted in the transition amplitude for $A = 117$ included in Fig. 11 and Table V. The points corresponding to the $19/2^+$, $E2$ isomeric decays in Fig. 11 also appear to exhibit a linear dependence with A and an average slope of $-1.0\,e\mathrm{fm}^2/A$; i.e., close to those discussed above. The fact remains, however, that the $B(E2)$ values are notably larger in magnitude than those observed for the $23/2^+$ isomers. This may arise from the more complex structure of these $19/2^+$ and $(15/2^+)$ states that involves amplitudes associated with both $(h_{11/2})^2 s_{1/2}$ and $(h_{11/2})^2 d_{3/2}$ configurations, where the latter component, apart from the $10^+ \rightarrow 8^+$ transition, also includes the $8^+ \rightarrow 6^+$ $E2$ transition. It is also worth pointing out that the zero crossing for these amplitudes appears to occur at $A = 121$ rather than at $A = 123$, the location of the half-filled $h_{11/2}$ subshell. However, further confirmation of these observations is desirable and must await the possible, future identification of the $19/2^+$ $E2$ decays in ^{119}Sn and ^{121}Sn. It should also be noted that the more complex structure of the $19/2^+$ state, discussed below in Sec. IV C, may affect the simple picture presented here for the $23/2^+ \rightarrow 19/2^+$ $B(E2)$ values. Although the linear behavior shown in Fig. 11 could not be reproduced by the calculations, it remains a tantalizing experimental observation.

B. Systematics of level energies

The systematics of level energies presented in Ref. [10] for a broad, $A = 116$–132 range of even-Sn isotopes exhibited a regular decrease with A in the excitation energies of the yrast states at any spin value. In fact, the observed regularity gave confidence in the assigned spin-parity values, and this turned out to be particularly helpful in the case of higher-seniority excitations. In Fig. 12, a similar systematics is presented for selected levels in the odd-A $^{119-125}$Sn isotopes, studied in the present work, and in $^{117,127-131}$Sn isotopes from earlier investigations [19–21,23]. Here, ^{131}Sn was added to illustrate the impact of the $N = 82$ shell closure in ^{132}Sn. In general, the regular lowering of level energies with increasing mass

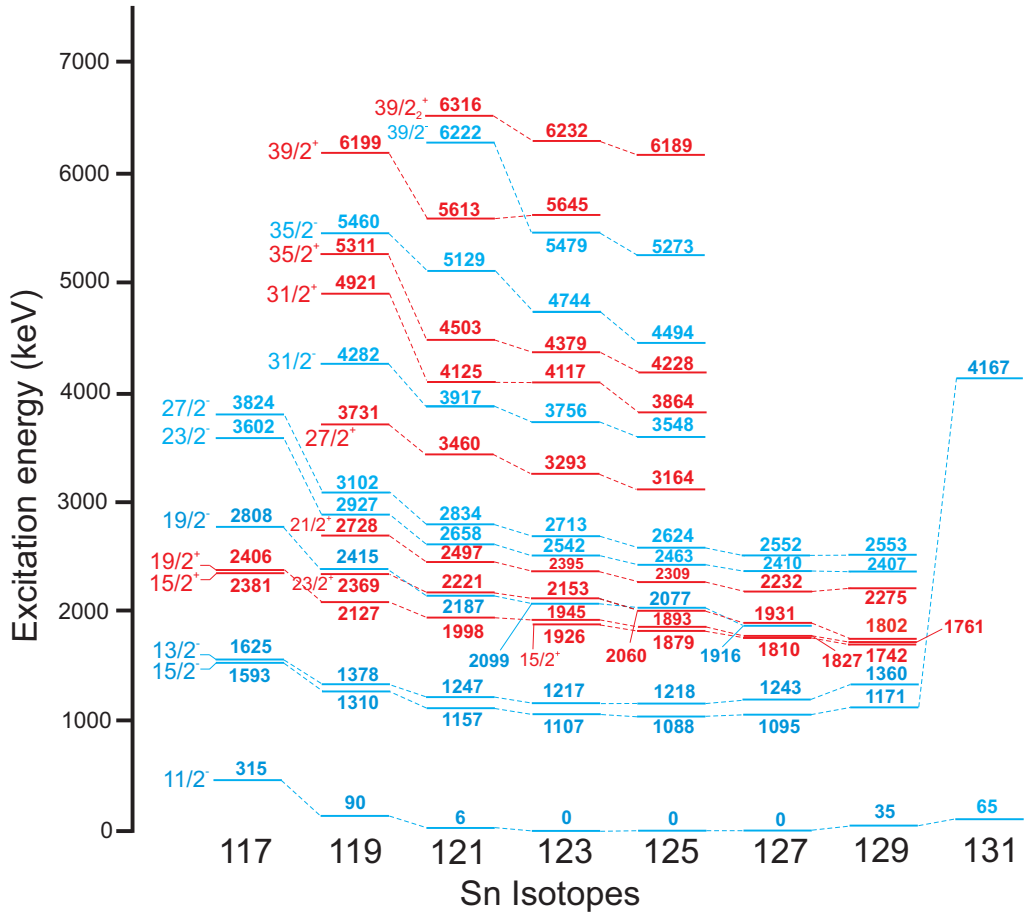

FIG. 12. Systematics of excitation energies of selected levels observed in a chain of neutron-rich odd Sn isotopes. For the sake of clarity, the positive-parity states have been marked in red while the negative-parity ones are given in blue. To highlight the $N = 82$ shell closure, the $15/2^-$ level in ^{131}Sn was also included.

number A follows the same trend as seen for the even isotopes. However, for some specific levels, the regular, smooth behavior does not happen to the extent that it can be used as strong confirmation of proposed spin-parity assignments. Note that, in Fig. 12, the level energies are plotted with respect to the respective ground states in order to also illustrate the A dependence of the $11/2^-$ levels as these become ground states only in the ^{123,125,127}Sn isotopes.

At variance with the trend noted for all other levels, the energy of the lowest $15/2^-$ and $13/2^-$ states, understood as arising from the coupling of the 2^+ core excitation with an $h_{11/2}$ neutron, is fairly stable with a shallow minimum around $A = 125$. This trend follows the behavior observed for the first 2^+ level in the even Sn isotopes, especially when considering energy spacings relative to the $11/2^-$ levels. All of the other states with seniority $\nu = 3$, up to the highest spin $27/2^-$ isomers, exhibit a regular energy lowering with increasing mass number, and this includes the new $23/2^+$ and $21/2^+$ levels, herewith supporting their spin-parity assignments. Here, one should also recall the remarkable similarity in the decay patterns populating both of these states from the $27/2^-$ isomer, systematically observed in all isotopes. A more dramatic lowering in excitation energies is observed for the seniority $\nu = 5$ levels in the four isotopes studied here. For the negative-parity $(31/2^-)$ and $(35/2^-)$ levels, the energy drops in a regular way and the same seems to hold for the tentatively assigned $(39/2^-)$ level which is likely a seniority $\nu = 7$ excitation. The positive-parity $(27/2^+)$, $(31/2^+)$, and $(35/2^+)$ states in general follow the same trend, however, in ^{121}Sn, the $(31/2^+)$ level is observed at a surprisingly low energy herewith partly altering the regularity. A similar situation is noted for the states assigned tentatively as $(39/2^+)$ levels. Here as well, the level energy in ^{121}Sn is significantly lower than expected on the basis of a smooth behavior to the extent that even a small rise in energy is observed for ^{123}Sn. In ^{121}Sn and ^{123}Sn, the present results also located tentatively assigned second $(39/2^+)$ states and these are included in Fig. 12. On the other hand, only one candidate $(39/2^+)$ level was established in ^{125}Sn and, from its excitation energy, it appears to be possibly related to the second $(39/2^+)$ states in the lighter isotopes.

C. Shell-model calculations

Shell-model calculations were carried out for all the odd-Sn isotopes discussed in the present work. For isotopes down to ^{123}Sn, the calculations were performed with the OXBASH code [24] using two-body matrix elements (TBMEs) taken from Ref. [25]. Starting with a ^{132}Sn closed core, the neutron holes can occupy the full valence space of $\nu(0g_{7/2}, 1d_{5/2}, 1d_{3/2}, 2s_{1/2}, 0h_{11/2})$ orbitals between the $N = 50$ and 82 major shells. The method is described in detail in Ref. [10], where it was previously employed for calculations of the excitation energies and configurations of states in the even-Sn isotopes. Here, it turned out that such calculations are quite time consuming and become particularly arduous for isotopes lighter than ^{123}Sn, as an increasing number of neutron holes is involved. Therefore, for ^{119}Sn and ^{121}Sn, the KSHELL code [26] was employed. Calculations with this code were found to be significantly faster. In this approach, the same TBMEs were used as in the OXBASH calculations, but neutron particles were considered rather than holes. They are assumed to fill the same subshells, but start from an ^{100}Sn closed core. For the heavier Sn isotopes, calculations with both codes gave equivalent results, although the KSHELL code does not provide information on the wave functions.

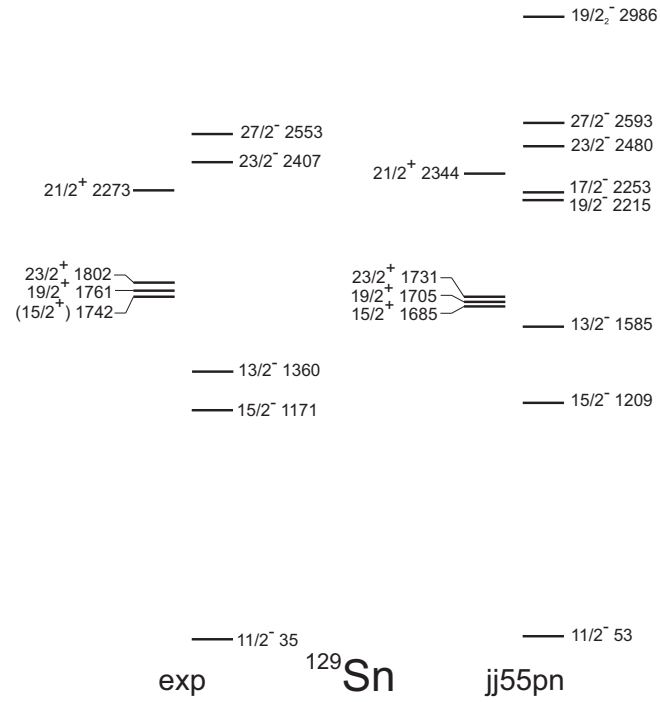

FIG. 13. Comparison between level energies established in the experiment and the results of shell-model calculations for the ^{129}Sn isotope. The negative- and positive-parity states are displaced with respect to one another to simplify the comparison.

In Figs. 13 and 14, comparisons between the experimental (left panel, labeled exp) and calculated (right panel, labeled jj55pn) excitation energies are displayed for the main yrast states in ^{129}Sn and ^{127}Sn, respectively. For both nuclei, calculations of seniority $\nu = 3$ levels are sufficient to cover the observed spin range which does not extend beyond the $27/2^-$ isomers. Nevertheless, for ^{127}Sn, results for computed $\nu = 5$ states are provided as well to illustrate the evolution of predicted excitation energies as a function of spin and parity. In both isotopes, the agreement between experiment and theory for the $\nu = 3$ levels is satisfactory, although in ^{127}Sn the calculated negative-parity states are lower than their experimental counterparts by more than 100 keV. A similar lowering of calculated energies was noted earlier in Ref. [10] for the $\nu = 2$ excitations in even-Sn isotopes. Despite the increasing complexity of the configurations involved, the general agreement between data and calculations is satisfactory as well in ^{125}Sn (Fig. 15), ^{123}Sn (Fig. 16), ^{121}Sn (Fig. 17), and ^{119}Sn (Fig. 18). Note that, with the exception of ^{129}Sn, the $11/2^-$ levels are calculated to be the ground states. Experimentally, however, they were established as low-lying isomers in ^{129,121,119}Sn, and in Figs. 13, 17, and 18 their

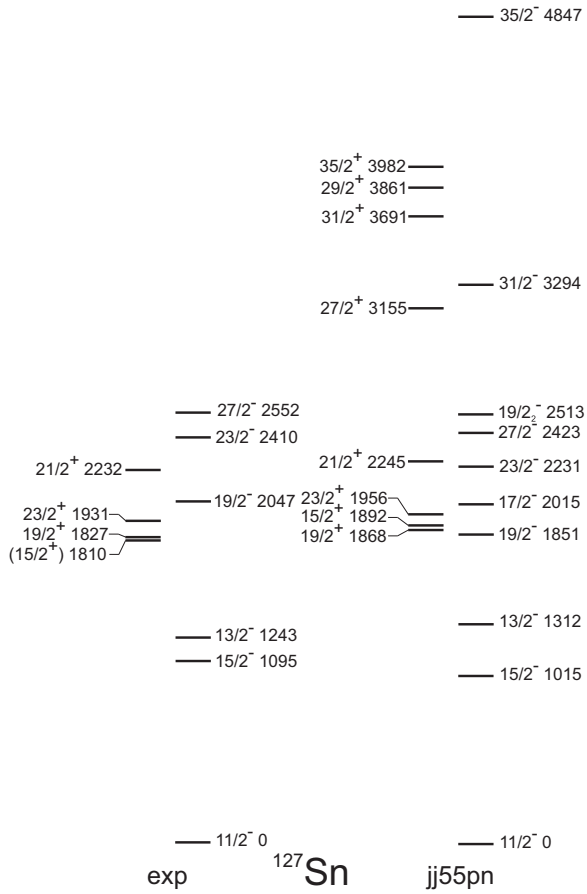

FIG. 14. Same as in Fig. 13, but for the ^{127}Sn isotope.

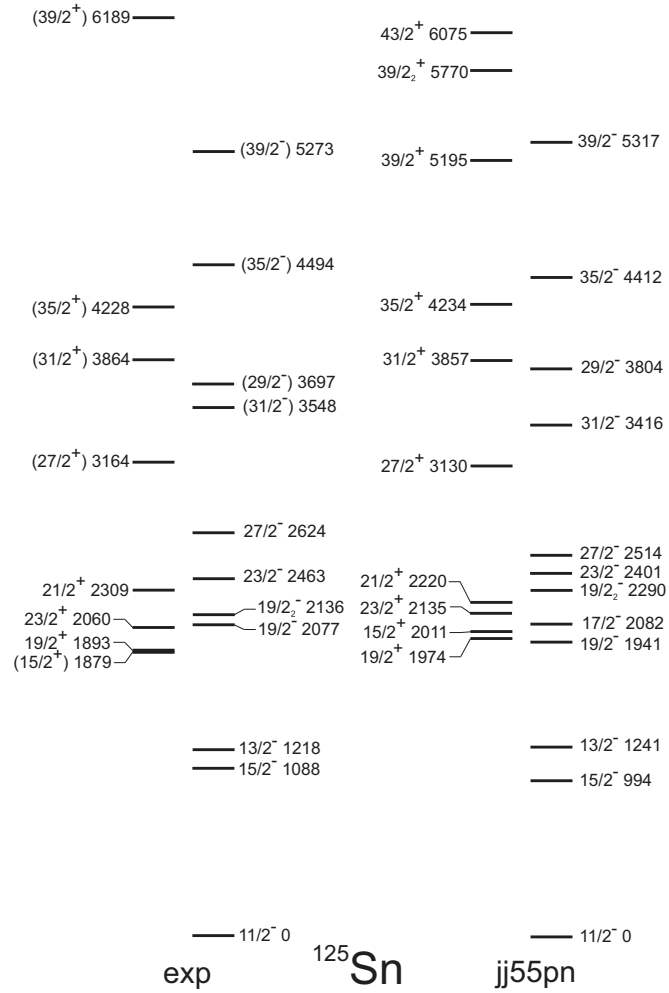

FIG. 15. Same as in Fig. 13, but for the ^{125}Sn isotope.

reported energies are indicated. Only in the case of ^{119}Sn (Fig. 18), where the excitation energy of the $11/2^-$ isomer is the largest (90 keV), have the computed energies been shifted upwards by the corresponding amount to avoid overstating the mismatch between data and calculations.

The seniority $\nu = 3$ highest-spin, $27/2^-$ states in all the odd neutron-rich isotopes considered in this work are characterized by a fairly pure $(h_{11/2})^3$ configuration: It contributes to the calculated wave functions with squared (in the following, for simplicity and easiness of reading, the word "amplitude" will be used rather than "squared amplitude") amplitudes larger than 90% for $^{129-123}$Sn (as indicated above, the KSHELL code, used for ^{121,119}Sn, does not readily provide information on the wave functions). The differences between the experimental and calculated excitation energies are rather small; they amount to 40, −129, −110, −103, −119, −198 keV in the $A = 129$–119 sequence of odd Sn isotopes. As mentioned above, differences of this size are also observed for other negative-parity states, and were also noted earlier in even isotopes [10]. The $23/2^-$ levels populated in the $27/2^-$ isomeric $E2$ decays, discussed in Sec. IV A, are also characterized by a dominant $(h_{11/2})^3$ configuration with respective wave-function amplitudes of 99%, 82%, 88%, and 86% in $^{129-123}$Sn. The $23/2^+$ ($\nu = 3$) isomers are unambiguously associated by shell-model calculations with the $(h_{11/2})^2 d_{3/2}$ configuration, although the calculated wave-function amplitudes decrease slowly from 97% in ^{129}Sn to 79% in ^{123}Sn. In the latter nucleus, and presumably also in the lighter isotopes, a more complex configuration applies that also involves neutron holes from the $s_{1/2}$ state as well as from the $g_{7/2}$ and $d_{5/2}$ orbitals which are farther removed from the Fermi surface. In general, the energies calculated for the $\nu = 3$, positive-parity levels are rather close to the experimental ones and the observed $19/2^+$ - $23/2^+$ - $21/2^+$ sequence of levels is reproduced well. A notable exception in this respect concerns the $15/2^+$ state which is calculated very close, yet above the $19/2^+$ isomer in the ^{127,125,123}Sn isotopes. In those isotopes, this $(15/2^+)$ level was observed in the decay of the $19/2^+$ isomers, as discussed in Sec. IV A. The assigned spin-parity values are hard to question on the basis of the calculations, especially because the only alternative, i.e., the $17/2^-$ level, was calculated to be located about 100 keV higher in energy. It should be noted that the structure of these $19/2^+$ isomers is quite different from that established for the $23/2^+$ states. Their main configuration involves unpaired $s_{1/2}$ and $d_{3/2}$ neutron holes. The calculations indicate that the $(h_{11/2})^2 d_{3/2}$ configuration contributes to the wave function with amplitudes of 80%, 52%, 36%, and 26%

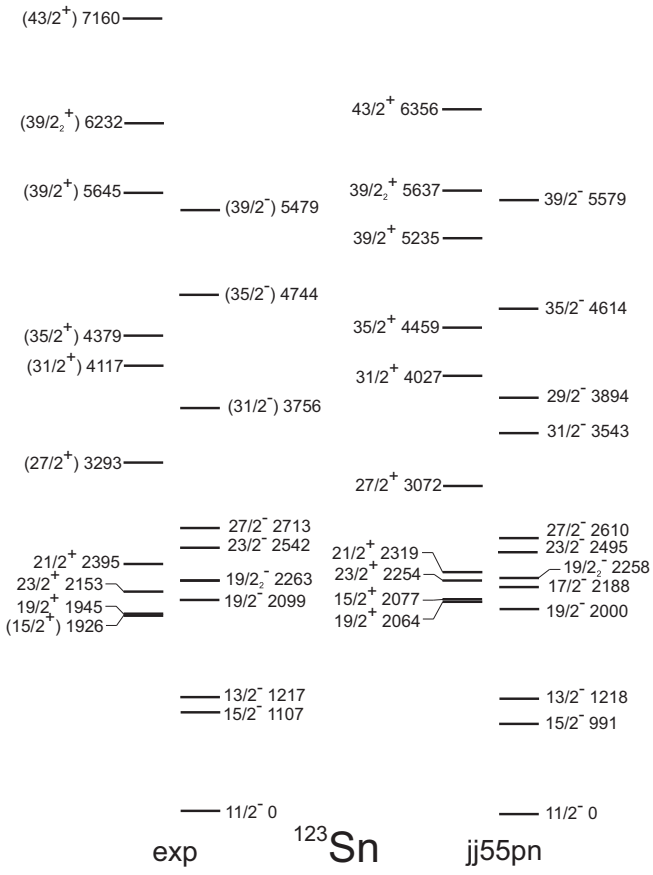

FIG. 16. Same as in Fig. 13, but for the ^{123}Sn isotope.

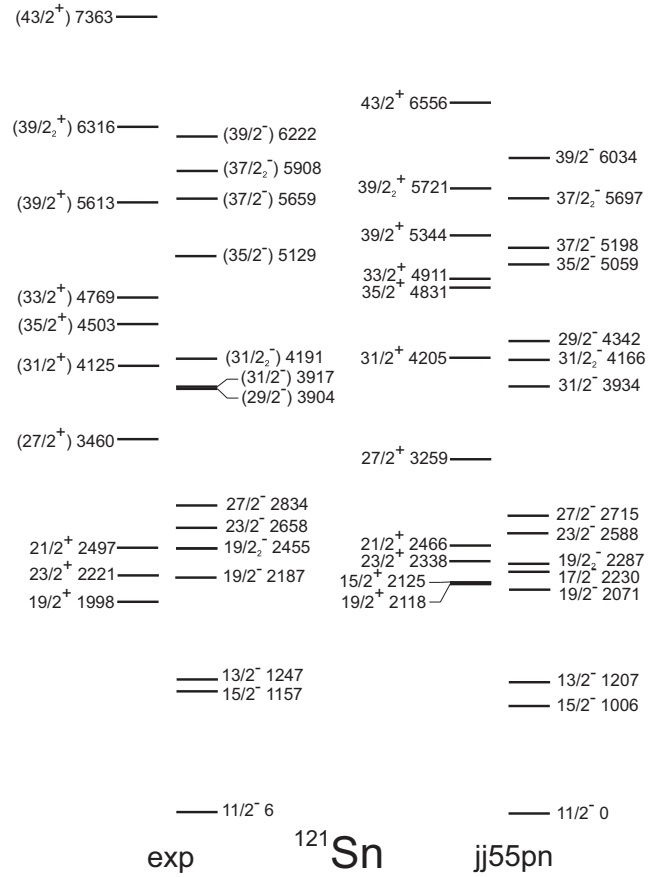

FIG. 17. Same as in Fig. 13, but for the ^{121}Sn isotope.

in the odd $^{129-123}$Sn isotopes, while the amplitudes of the $(h_{11/2})^2 s_{1/2}$ configuration are 16%, 46%, 56%, and 47% for the same sequence of isomers. A similar configuration with sizable $(h_{11/2})^2 d_{3/2}$ and $(h_{11/2})^2 s_{1/2}$ components characterizes the $15/2^+$ levels fed from the $19/2^+$ isomers. As discussed in Sec. IV A, the larger $B(E2)$ values for these $19/2^+ \rightarrow (15/2^+)$ $E2$ transitions compared to those seen for the $23/2^+ \rightarrow 19/2^+$ decays may reflect the contribution of the $(h_{11/2})^2 d_{3/2}$ component that enables the involvement of the $8^+ \rightarrow 6^+$ $(h_{11/2})^2$ $E2$ transition only in the former case.

The $E2$ branching observed in the decay from $23/2^-$ states in ^{121,123,125}Sn toward two $19/2^-$ levels is noteworthy. The initial state is characterized by a well-defined $(h_{11/2})^3$ dominant configuration, and one would, *a priori*, expect the $E2$ decay to populate preferentially the $19/2^-$ level with the same character. A less intense branch would then feed the $19/2^-$ state with a more complex wave function involving a single, unpaired $h_{11/2}$ neutron hole together with other holes in positive-parity orbitals able to couple to the required 4 units of spin. The measured energies and intensities of the observed $E2$ branches were used to calculate $B(E2)$ ratios for the transitions feeding the $19/2_1^-$ and $19/2_2^-$ states, yielding ratios of 0.69, 0.03, and 1.89 in ^{121,123,125}Sn, respectively. From these measured values, it is clear that only in the case of ^{123}Sn is the $19/2_2^-$ level strongly preferred, and that a large mixing between configurations must occur in the other cases.

In these ^{121,123,125}Sn isotopes, the shell-model calculations indeed predict two $19/2^-$ states at energies close to the data (see Figs. 15–17). Moreover, the much higher calculated energy for the $19/2_2^-$ levels in ^{129}Sn (Fig. 13) and ^{127}Sn (Fig. 14) accounts for the fact that, in those nuclei, these states were not observed. On the other hand, in ^{119}Sn, the two $19/2^-$ states were calculated to be separated by about 300 keV, yet, only the yrast state was seen. It is possible that, in this case, the large difference in $23/2^- \rightarrow 19/2^-$ transition energies results in a somewhat weak $E2$ branch toward the $19/2_2^-$ state, i.e., below the detection limit. Whereas the calculated energy separation between the two $19/2^-$ levels in ^{121}Sn agrees well with experiment, in ^{123}Sn and particularly in ^{125}Sn, the experimental splitting is significantly smaller than the computed one. This may indicate that, in the heavier isotopes, the real mixing between the $19/2^-$ states is less effective than implied by the calculations. The wave-function amplitudes confirm the complex composition of both $19/2^-$ levels, but also indicate a clear shift of the main $(h_{11/2})^3$ component from the $19/2_1^-$ to the $19/2_2^-$ state in the lighter isotopes. In ^{129}Sn, the two $19/2^-$ levels have distinct configurations: The $19/2_1^-$ state has a wave function with a 90% amplitude for the $(h_{11/2})^3$ configuration, while the $19/2_2^-$ one is characterized by an unpaired $h_{11/2}$ hole coupled to deeper-lying neutron holes with an 85% amplitude. As a result, this latter level is calculated to be located at much higher excitation energy.

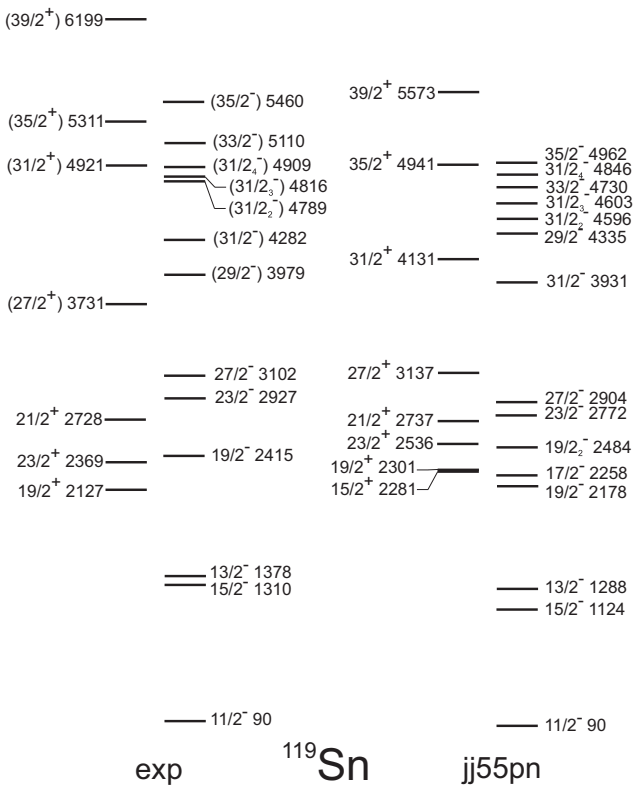

FIG. 18. Same as in Fig. 13, but for the ^{119}Sn isotope. The theoretical values have been offset by 90 keV (see text for details).

In ^{127}Sn, the $19/2^-_1$ level has only a 68% contribution from the $(h_{11/2})^3$ configuration while the one with the unpaired $h_{11/2}$ hole has a 28% amplitude. The contribution of the pure $(h_{11/2})^3$ configuration in the $19/2^-_1$ state continues to decrease systematically for the lighter isotopes and reaches 45% for ^{123}Sn while the involvement from the other orbitals increases. The opposite situation occurs for the $19/2^-_2$ levels: Here the contribution by the $(h_{11/2})^3$ configuration increases significantly in the lighter isotopes and reaches an amplitude of 70% for ^{123,125}Sn. In view of this systematic picture emerging from the calculations, the remarkably small experimental $B(E2)$ ratio that strongly favors the $19/2^-_2$ population in ^{123}Sn can hardly be explained on the basis of differing intrinsic structures for both $19/2^-$ states. Rather, it can likely be attributed to the special situation where the $h_{11/2}$ orbital is half-filled in this nucleus, a situation resulting in $B(E2)$ values for transitions between states associated with the $(h_{11/2})^3$ configuration being very small.

For the positive-parity, seniority $\nu = 5$ states, shell-model calculations only partially reproduce the experimental data throughout the isotopic chain. In the case of ^{125}Sn, the agreement is satisfactory with calculated $27/2^+$, $31/2^+$, and $35/2^+$ states merely 34, 7, and 6 keV removed from their experimental counterparts. However, in the lighter isotopes, the computed energies are generally too low and a rather dramatic discrepancy occurs for ^{119}Sn. Here, these positive-parity states are calculated at energies up to 800 keV lower than the data. At present, the reason for this mismatch is not understood. It is conceivable that theory overestimates contributions from neutron holes occupying orbitals far removed from the Fermi surface in the case of the $27/2^+$ and $31/2^+$ states but, on the other hand, the wave functions for the $35/2^+$ levels indicate contributions in excess of 80% from the $(h_{11/2})^4 d_{3/2}$ configuration with maximally aligned spin.

A more satisfactory agreement between experiment and theory is observed for the $\nu = 5$ negative-parity levels, although, again, the calculations for most states are too low in ^{119}Sn. The yrast $31/2^-$ and $35/2^-$ levels involve mainly the $(h_{11/2})^5$ configuration, with wave-function amplitudes of about 50% in all cases. The calculated energies match their experimental counterparts well, herewith confirming the proposed spin-parity assignments. The situation with the $(29/2^-)$ states is less clear: These levels were identified in all the isotopes under investigation, except in ^{123}Sn. The $29/2^-$ calculated energies exhibit a trend opposite that seen for other states, as they are predicted higher than the data by as much as 438 keV in ^{121}Sn. Nevertheless, the calculations validate the proposed $29/2^-$ spin-parity assignments. Apart from the $(31/2^-)$ yrast states, one and three $(31/2^-)$ nonyrast levels have been established in ^{121}Sn and ^{119}Sn, respectively. Although the computed energies do not match the data as well as in other instances, the calculations clearly predict, respectively, two and four $31/2^-$ levels in these isotopes within the energy range corresponding to $\nu = 5$ excitations. The presence of these additional levels also confirms the expectation of an increasing complexity in the level structure above the $27/2^-$ isomers in lighter Sn isotopes. This was discussed in Sec. III A, where it helped to understand this part of the ^{119}Sn level scheme.

With the exception of the $\nu = 5$, $39/2^+$ state associated with the $(h_{11/2})^4 g_{7/2}$ configuration, all other $\nu = 5$ excitations must have spin values of 35/2 or less. Hence, the observed states with higher spin correspond to more complex excitations with seniority $\nu = 7$. Only a few such states could be identified in the present study as the population in fission drops somewhat abruptly at high angular momentum and excitation energy. Among these, the $(39/2^-)$ $\nu = 7$ excitations are the negative-parity levels with the highest spin observed in three isotopes and their energies are reproduced rather well by the calculations. In the case of ^{125}Sn and ^{123}Sn, the computed states are located 44 and 100 keV above the experimental ones, respectively, while for ^{121}Sn, the $(39/2^-)$ level is computed only 188 keV too low. The associated wave functions reveal a main contribution by the $(h_{11/2})^5$ configuration coupled to 2^+ excitations from neutron holes distributed over all the positive-parity orbitals with the $g_{7/2}$ orbital playing an increasing role for the lighter isotopes. Also, in the high-spin region, several positive-parity states were established, albeit with tentative quantum numbers. While, in ^{119}Sn and ^{125}Sn, only a single $(39/2^+)$ level was observed, two such states were established together with a single $(43/2^+)$ level in ^{121}Sn and ^{123}Sn. Although the calculated energies for these states follow the general trend noted for other positive-parity levels and are significantly lower than the corresponding data, the structure of the yrast $39/2^+_1$ level is dominated, as expected, by the $\nu = 5\,(h_{11/2})^4 g_{7/2}$ configuration. Indeed, the wave functions for this $39/2^+_1$ state in ^{127,125,123}Sn attribute 100%, 82%, and 67%

amplitudes to this configuration. Only in ^{125}Sn was a $(39/2^+_2)$ level observed as well. It is clear that this nonyrast level must involve the $(h_{11/2})^6 d_{3/2}$ and more complex configurations which can then also produce the $(43/2^+)$ state.

Finally, a short comment should be devoted to the 4769-keV level located just above the $(35/2^+)$ state and observed only in ^{121}Sn. The low-energy, 266-keV transition connecting this level with the $(35/2^+)$ state of $(h_{11/2})^4 d_{3/2}$ character is reminiscent of the $14^- \rightarrow 15^-$ decays observed and discussed in the study of the even Sn isotopes of Ref. [10]. In ^{121}Sn, the absence of any feeding into this state from higher-lying levels supports a spin value lower than $35/2^+$. Furthermore, the shell-model calculations predict a $33/2^+$ level at an energy close to the experimental value (see Fig. 17). One may thus conclude that, indeed, this level represents the $(I_{\max}\text{-}1)$ coupling of the $(h_{11/2})^4 d_{3/2}$ configuration, in analogy with the 14^- states observed in several even Sn isotopes. Despite extensive searches, such a level could not be observed in the other odd Sn isotopes.

V. CONCLUSIONS

Neutron-rich, odd Sn isotopes with $A = 119$–125 have been investigated as a continuation of the study of even Sn nuclei presented earlier in Ref. [10]. All these isotopes were populated by fission following reactions of ^{48}Ca and ^{64}Ni beams with ^{208}Pb and ^{238}U targets. The analysis of the prompt and delayed coincidence data collected with the Gammasphere array in three measurements extended significantly the high-spin level schemes in the broad range where seniority $\nu = 3$, 5, and 7 excitations occur in the four odd Sn isotopes. The experimental information on the $\nu = 3$ states was completed through several new findings, including the first identification of the $23/2^+$ isomer in ^{119}Sn and the confirmation of this isomer in ^{121}Sn. In all these odd isotopes, the decay branches from the $27/2^-$ isomers to the $21/2^+$ and $23/2^+$ states were delineated. In the higher-spin parts of the level schemes, extensive structures of negative-parity levels were identified above the $27/2^-$ isomers, up to the $(39/2^-)$, $\nu = 7$ excitation. In each case, a sequence of positive-parity states was established with the yrast $(35/2^+) \rightarrow (31/2^+) \rightarrow (27/2^+) \rightarrow 23/2^+$ $E2$ cascades feeding the $23/2^+$ isomers. Furthermore, in ^{123}Sn, a short half-life could be determined for the $(35/2^+)$ state. Above the $(35/2^+)$ levels, higher-spin $(39/2^+)$ states were located, and in the ^{121,123}Sn isotopes the $(43/2^+)$ level could be observed as well.

In the discussion of the results, the previously known level schemes of ^{117,127,129}Sn were included in the systematics of level energies and $B(E2)$ reduced transition probabilities, thus covering the $A = 117$–129 range. The regular decrease of the level energies with A mirrors the trend established for the even Sn nuclei [10] and this systematics gives further confidence to the spin-parity assignments proposed on the basis of the experimental results. The systematics of the $B(E2)$ amplitudes for the $E2$ decays of isomeric $23/2^+$ and $19/2^+$ states follow the general trend established for the $(h_{11/2})^n$ seniority $\nu = 2$, 3 isomers as well as for the $\nu = 4$, 13^- and 15^- isomers seen in even Sn isotopes [10]. In the case of $19/2^+$ states, some noted differences were discussed in terms of the mixing of configurations involving the $s_{1/2}$ and $d_{3/2}$ orbitals.

Shell-model calculations were carried out for all of the $^{119-129}$Sn isotopes and, for most of the experimental levels, the computed energies agree rather well with the data. Some systematic differences were pointed out, in particular for the high-spin, positive-parity levels. These may serve as guidance for improvements of some of the input parameters in future calculations. The interpretation of the level structures was discussed with support from the calculated wave functions. The present work completes the study of high-spin states in the neutron-rich Sn isotopes. It confirms the adequacy of the shell model for the quantitative description of the observed states. However, it also provides data that may help improve the accuracy of such calculations further.

ACKNOWLEDGMENTS

The authors thank the ATLAS operating staff for the efficient running of the accelerator and J. P. Greene for target preparations. We are indebted to B. Szpak for his advice in conducting the theoretical calculations. This work was supported by the Polish National Science Center, Projects No. UMO-2012/07/N/ST2/02861, the U.S. Department of Energy, Office of Nuclear Physics, under Contract No. DE-AC02-06CH11357 (A.N.L.) and Grant No. DE-FG02-94ER40834 (U.M.). This research used resources of ANL's ATLAS facility, a DOE Office of Science User Facility.

[1] M. Ogawa, R. Broda, K. Zell, P. J. Daly, and P. Kleinheinz, Phys. Rev. Lett. **41**, 289 (1978).
[2] J. H. McNeill, J. Blomqvist, A. A. Chishti, P. J. Daly, W. Gelletly, M. A. C. Hotchkis, M. Piiparinen, B. J. Varley, and P. J. Woods, Phys. Rev. Lett. **63**, 860 (1989).
[3] P. J. Daly, P. Klenheinz, R. Broda, S. Lunardi, H. Backe, and J. Blomqvist, Z. Phys. A **298**, 173 (1980).
[4] M. Ishihara, R. Broda, and B. Herskind, in *Proceedings of the International Conference on Nuclear Physics*, Munich, Vol. 1, edited by J. de Boer and H. J. Mang (North-Holland, Amsterdam, 1973), p. 256.
[5] R. Broda, R. H. Mayer, I. G. Bearden, P. Benet, P. J. Daly, Z. W. Grabowski, M. P. Carpenter, R. V. F. Janssens, T. L. Khoo, T. Lauritsen, E. F. Moore, S. Lunardi, and J. Blomqvist, Phys. Rev. Lett. **68**, 1671 (1992).
[6] R. H. Mayer *et al.*, Phys. Lett. B **336**, 308 (1994).
[7] C. T. Zhang, P. Bhattacharyya, P. J. Daly, Z. W. Grabowski, R. Broda, B. Fornal, and J. Blomqvist, Phys. Rev. C **62**, 057305 (2000).
[8] S. Lunardi, P. J. Daly, F. Soramel, C. Signorini, B. Fornal, G. Fortuna, A. M. Stefanini, R. Broda, W. Meczyński, and J. Blomqvist, Z. Phys. A **328**, 487 (1987).
[9] Y. H. Chung, P. J. Daly, H. Helppi, R. Broda, Z. W. Grabowski, M. Kortelahti, J. McNeill, A. Pakkanen, P. Chowdhury, R. V. F. Janssens, T. L. Khoo, and J. Blomqvist, Phys. Rev. C **29**, 2153 (1984).

[10] Ł. W. Iskra, R. Broda, R. V. F. Janssens, J. Wrzesiński, B. Szpak, C. J. Chiara, M. P. Carpenter, B. Fornal, N. Hoteling, F. G. Kondev, W. Królas, T. Lauritsen, T. Pawłat, D. Seweryniak, I. Stefanescu, W. B. Walters, and S. Zhu, Phys. Rev. C **89**, 044324 (2014).
[11] A. Astier, M.-G. Porquet, C. Theisen, D. Verney, I. Deloncle, M. Houry, R. Lucas, F. Azaiez, G. Barreau, D. Curien, O. Dorvaux, G. Duchêne, B. J. P. Gall, N. Redon, M. Rousseau, and O. Stézowski, Phys. Rev. C **85**, 054316 (2012).
[12] I. Y. Lee, Nucl. Phys. A **520**, 641c (1990).
[13] R. Broda, J. Phys. G: Nucl. Part. Phys. **32**, R151 (2006).
[14] R. Broda, T. Pawłat, W. Królas, R. V. F. Janssens, S. Zhu, W. B. Walters, B. Fornal, C. J. Chiara, M. P. Carpenter, N. Hoteling, Ł. W. Iskra, F. G. Kondev, T. Lauritsen, D. Seweryniak, I. Stefanescu, X. Wang, and J. Wrzesiński, Phys. Rev. C **86**, 064312 (2012).
[15] W. Królas, R. Broda, B. Fornal, R. V. F. Janssens, A. Gadea, S. Lunardi, J. J. Valiente-Dobon, D. Mengoni, N. Mărginean, L. Corradi, A. M. Stefanini, D. Bazzacco, M. P. Carpenter, G. De Angelis, E. Farnea, E. Fioretto, F. Galtarossa, T. Lauritsen, G. Montagnoli, D. R. Napoli, R. Orlandi, T. Pawłat, I. Pokrovskiy, G. Pollarolo, E. Sahin, F. Scarlassara, D. Seweryniak, S. Szilner, B. Szpak, C. A. Ur, J. Wrzesiński, and S. Zhu, Phys. Rev. C **84**, 064301 (2011).
[16] Ł. W. Iskra *et al.*, Acta Phys. Pol. B **44**, 395 (2013).
[17] Ł. W. Iskra *et al.*, Acta Phys. Pol. B **46**, 651 (2015).
[18] R. H. Mayer *et al.*, Z. Phys. A **342**, 247 (1992).
[19] R. L. Lozeva *et al.*, Phys. Rev. C **77**, 064313 (2008).
[20] J. A. Pinston, C. Foin, J. Genevey, R. Béraud, E. Chabanat, H. Faust, S. Oberstedt, and B. Weiss, Phys. Rev. C **61**, 024312 (2000).
[21] O. Hashimoto, Y. Shida, G. Ch. Madueme, N. Yoshikawa, M. Sakai, and S. Ohya, Nucl. Phys. A **318**, 145 (1979).
[22] J. Blomqvist, in *International Review of Nuclear Physics*, Vol. 2 (World Scientific, Singapore, 1984), pp. 1–32.
[23] P. Bhattacharyya, P. J. Daly, C. T. Zhang, Z. W. Grabowski, S. K. Saha, R. Broda, B. Fornal, I. Ahmad, D. Seweryniak, I. Wiedenhöver, M. P. Carpenter, R. V. F. Janssens, T. L. Khoo, T. Lauritsen, C. J. Lister, P. Reiter, and J. Blomqvist, Phys. Rev. Lett. **87**, 062502 (2001).
[24] B. A. Brown, A. Etchegoyen, N. S. Godwin, W. D. M. Rae, W. A. Richter, W. E. Ormand, E. K. Warburton, J. S. Winfield, L. Zhao, and C. H. Zimmerman, "OXBASH for Windows," MSU-NSCL Report 1289 (Michigan State University–National Superconducting Cyclotron Laboratory, East Lansing, 2004).
[25] B. A. Brown, N. J. Stone, J. R. Stone, I. S. Towner, and M. Hjorth-Jensen, Phys. Rev. C **71**, 044317 (2005).
[26] N. Shimizu, arXiv:1310.5431.